Chandra Pandey

Application of Printing Techniques in Hybrid Photovoltaic Technologies

Helsinki Metropolia University of Applied Sciences

Bachelor of Engineering

Media Engineering

Thesis

18th April 2015

Metropolia

Author(s) Title Number of Pages Date	Chandra Pandey Application of Printing Techniques in Hybrid Photovoltaic Technologies 50 pages + 3 appendices 18th April 2015
Degree	Bachelor of Engineering
Degree Programme	Media Engineering
Specialization option	Hybrid Media , Technology Business
Instructor(s)	Aarne. Klemetti, Senior Lecturer Dr. M. I. Asghar, Senior Research Coordinator

In this work application of various printing technologies in different kinds of photovoltaic technologies are studied. Photovoltaic technologies are generally classified intro three generations. A brief literature overview of various photovoltaic technologies belonging to these generations is presented. After explaining the basics of different types of photovoltaic technologies, a list of printing technologies are first introduced and then their application in different photovoltaic technologies is explained.

The printing technologies that were covered in final year work include screen printing, inkjet printing, laser printing, thermal evaporation, sputtering, chemical vapor deposition, electrochemical deposition, spin coating, photolithography, nanoimprinting, electrophotography, lamination technology, sheet-fed printing, web printing, gravure and 3-dimentional printing.

In the experimental part, three different photovoltaic technologies, i.e. crystalline silicon solar cells, organic solar cells and dye-sensitized solar cells which utilize different kinds of printing technologies during their manufacturing, were measured under standard measurement condition, i.e. 1000 W/m^2 AM1.5G equivalent light intensity at room temperature. Performance parameters of solar cells i.e. short-circuit-current-density, open circuit voltage and fill factors were obtained and finally the efficiencies of the solar cells, were calculated. The efficiencies for crystalline silicon solar cell, organic solar cell and dye-sensitized solar cell were 14.5%, 5.9% and 4.2% respectively.

All the three generations of solar cells have benefited from the versatile printing technologies. Many of the manufacturing challenges are solved by the development of new printable materials and the easy to up-scale methods of printing.

Keywords	hybrid, nanotechnology, photovoltaic, printing, solar

Contents

List of Abbreviations

AM	Air Mass
CVD	Chemical vapor deposition
EU	European Union
FF	Fill factor
FTO	Fluorine doped tin oxide
GW	Gigawatt
IEA	International Energy Agency
IPCC	Intergovernmental Panel on Climate Change
IPCE	Incident photon to current conversion efficiency
I_{SC}	Short current density
ITO	Indium doped tin oxide
IV	Current-voltage
KW	Kilowatt
MW	Megawatt
MENA	Middle Eastern and North African countries
PV	Photovoltaic
PVD	Physical vapor deposition
TCO	Transparent conduction oxide

V_{OC}	Open circuit voltage
η	Photovoltaic efficiency
3D	3 dimensional
Ω	Omega
θ	Theta

1 Introduction

Energy is arguably the biggest challenge humanity is facing today. Annual global energy demand is increasing rapidly every year. It is estimated that the global energy demand will increase to 16 terawatt (TW) in the year 2030 from 13 terawatt (TW) in 2013 [1]. Today about 85% of the global energy demand is fulfilled by fossil fuels [1]. The current energy sources are depleting and also causing environmental pollution. According to an inter-governmental panel on climate change, 60-80% reduction in carbon emission is needed to limit the climate change [1]. Therefore, there is a huge demand of clean energy sources as shown in Figure 1.

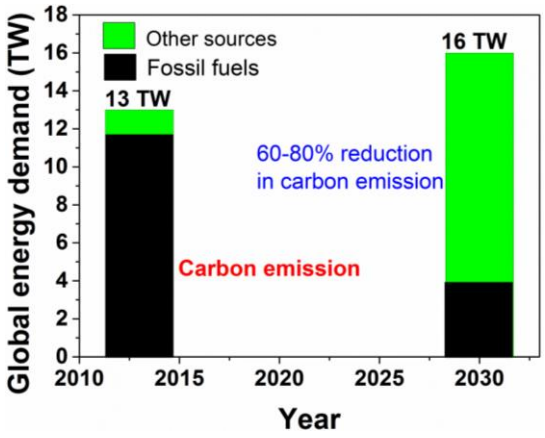

Figure 1. Global energy demand in terms of fossil fuels and other clean energy sources Reprinted from Pandey (2014) [2].

Photovoltaic (PV) solar cells are reliable, sustainable, natural and environmentally friendly energy technology. In the year 2014, the annual production of photovoltaic cells reached around 39.8 gigawatts (GW) [3] and is expected to grow much more in the future. Solar power is already a $150 billion business; with some 138 gigawatt (GW) of photovoltaic (PV) capacity already in place [3] the total global PV installments are expected to reach 400 GW by 2020 [3]. Finland is renowned in the world for its technological strength and commitment for clean environment. Finland has the biggest solar power plant (also known as solar park) in the Nordic region with a capacity of ~0.4 MW.

Due to huge business potential, many big companies have started investing in the PV industry which is booming at the moment and will continue to boom for at least for the next 20 years. At the moment, there are many manufacturers fiercely competing with

each other in terms of performance of their solar panel to the price ratio. The intense competition drives companies to seek ever new and more effective materials and solutions for solar panels. Recently, the PVTECH Magazine (2013) [4] ranked the top leading photovoltaic panel manufacturers in the world according to panel performance in the following order: Yingli Green Energy, Trinia Solar, Sharp Solar, Canadian Solar, Jinko Solar, Rene Solar, First Solar, Hanwha Solar One, Kyocera and JA Solar. In order to outperform the competitors in the PV market, it is necessary to optimize the panel design and manufacturing processes. If the manufacturing process of the solar panels can be made easy to scale up using printing technologies, mass production of the solar panels will be possible at a significantly lower cost as compared to the conventional standard manufacturing methods.

The PV technology, despite its tremendous growth, is facing certain challenges, which hinder its usage for many applications. These challenges can be partly or fully solved by the recent developments in the printing technologies. In this work, application of wide a variety of printing technologies in PV technologies is presented and it is anticipated that future progress of PV technologies is coupled with the advancement in printing technologies.

In the first chapter of this thesis, an introduction and motivation for the thesis is briefly presented. In the second chapter a literature overview of different PV technologies is given, followed by the applications of various printing technologies in the PV systems. In the third chapter, experimental details of the practical work done in this thesis are given. Chapter 3 includes both manufacturing and measurements of the solar cells. In the fourth chapter, the measurements results are discussed and analyzed. Finally in the fifth chapter, conclusions are presented.

2 Theoretical background

2.1 Performance parameters of photovoltaic technology

The performance of a photovoltaic cell is represented by its efficiency (η) of converting incoming light into electric current under standard reporting conditions (SRC). Generally PV cells are measured under AM1.5G or AM1.5D conditions. AM stands for air mass and is given by Eq. 1 [5]:

$$AM = \frac{1}{cos\theta} = \frac{Y}{X} \quad (1)$$

Where θ is the angle between the vertical or the zenith and the sun, X and Y are the light overhead path length, i.e. θ=0°, and certain path length in air atmosphere, i.e. θ=θ, respectively as shown in Figure 2.

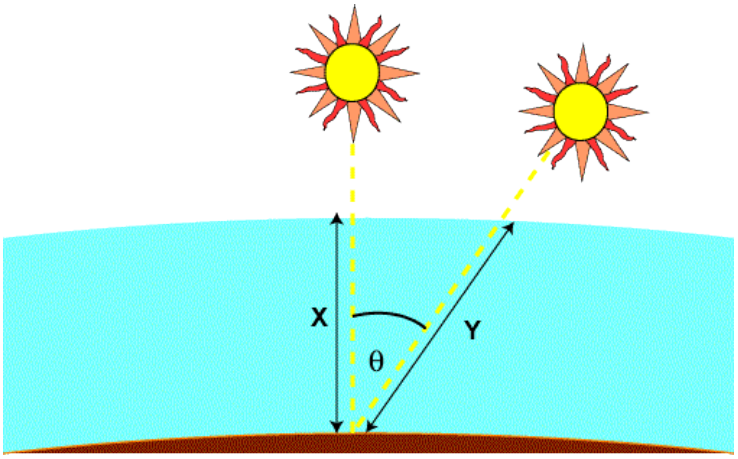

Figure 2. Air mass as a function of angle θ between the zenith and the sun. Reprinted from PV Education.org [5].

When the sun is at an angle of approximately 48°, the ratio of Y/X is 1.5 and the value of AM becomes 1.5. AM1.5G takes into account both the direct and indirect sunlight, whereas AM1.5D takes into account only direct sunlight and neglects the indirect light from the surroundings. Mostly, the performance is measured at a light intensity of 1000 W/m^2 with AM1.5G spectrum at 25°C and also referred as 1 Sun.

In practice the efficiency of a PV cell is calculated by measuring its current-voltage curve under 1 Sun equivalent conditions in a solar simulator machine. A typical IV curve of a PV cell is shown in Figure 3.

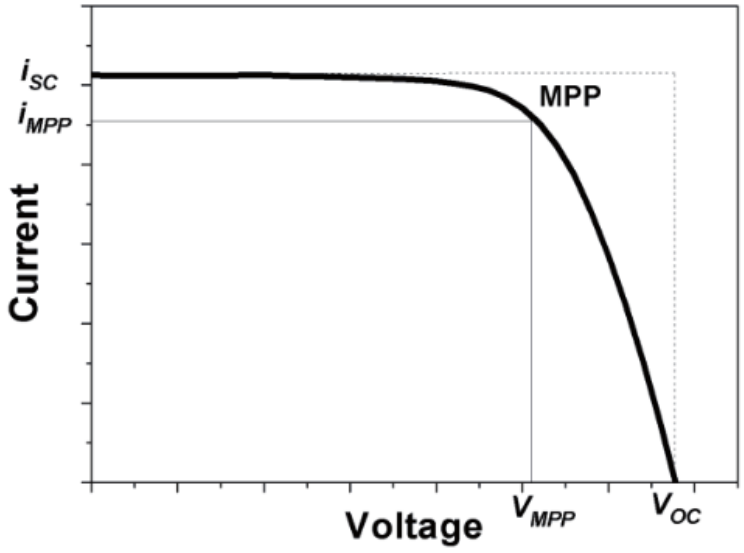

Figure 3. Typical IV curve of a PV cell and its performance parameters. Reprinted from Asghar (2012) [1].

From the IV curve, important performance parameters are obtained which include short current density (I_{SC}), open circuit voltage (V_{OC}) and fill factor (FF). The FF is calculated using Eq. 2 [1].

$$FF = \frac{V_{MPP}\, i_{MPP}}{I_{SC}\, V_{OhC}} \tag{2}$$

Where V_{MPP} and i_{MPP} are the voltage and current at maximum power point respectively. The maximum power delivered by a PV cell is given by Eq. 3 [1].

$$P_{MAX} = V_{MPP}\, I_{MPP} \tag{3}$$

The P_{MAX} can be expressed in terms of fundamental performance parameters as given by Eq. 4 [1].

$$P_{MAX} = V_{OC}\, I_{SC}\, FF \tag{4}$$

The efficiency of a PV cell is given as a ration between the maximum power generated by it and the power of the incident light (P_{IN}) [1].

$$\eta = \frac{P_{MAX}}{P_{IN}} \quad (5)$$

The P_{IN} is a product of intensity of light (I) and the area of the PV cell (A) under measurement. Finally, the efficiency of a PV cell is given by Eq. 6 in terms of its fundamental performance parameters [1].

$$\eta = \frac{V_{OC}\, I_{SC}\, FF}{I\, A} \quad (6)$$

The efficiency of a solar cell may decrease due to three major loss mechanisms:

1. Series resistance (Rs)
2. Shunt resistance (Rsh)
3. Recombination (radiation, single-level trap, auger)

The series resistance is due to ohmic losses. The interfaces at the electrical contacts are major reasons for ohmic losses. The shunt resistance is due to leakage currents. The recombination results in loss of charge carriers i.e. electrons and holes. The effects of the series and shunt resistance loss mechanisms on the IV curves are shown in Figure 4 and 5. The recombination losses mainly affect the fill factor of the IV curves. [11].

A major effect of series resistance appears on the slope of the IV curve near the open circuit voltage. In case of an ideal solar cell in which there is no series resistance, the slope near the open circuit voltage is very high. In this case the fill factor of the solar cells is also very high.

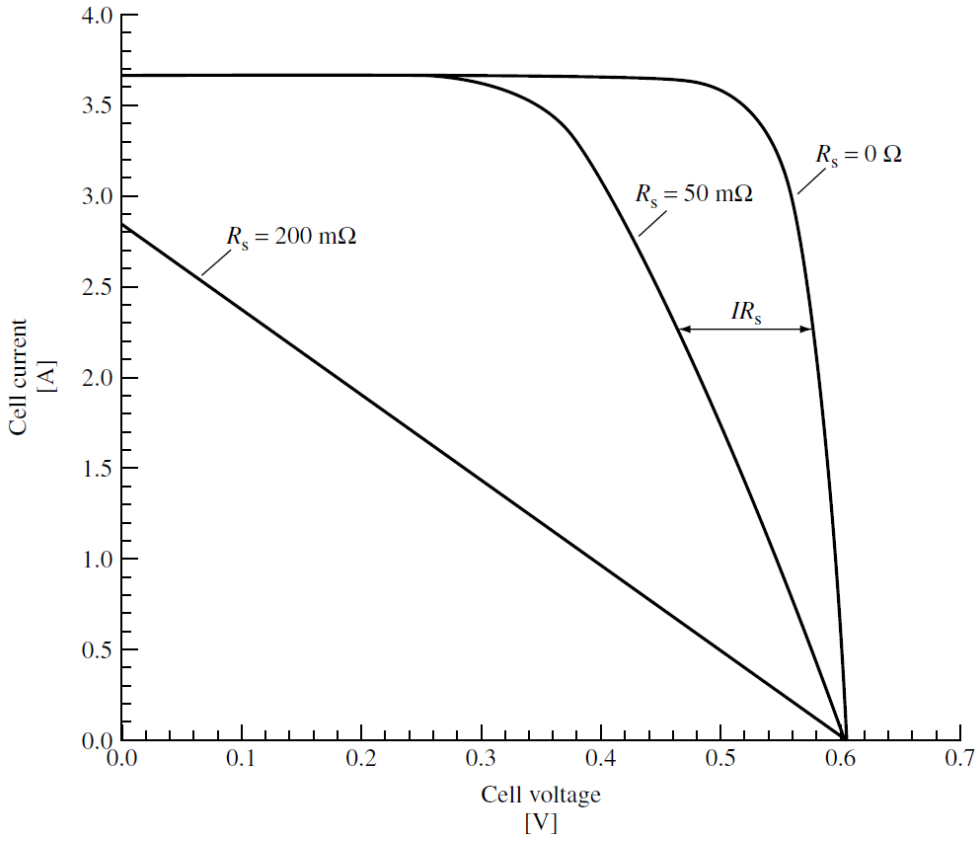

Figure 4. Effect of series resistance on the current-voltage curve of a solar cell. Reprinted from Luque and Hegedus (2003) [6,11].

As the series resistance increases, the slope near the open circuit voltage decreases accordingly. For instance, the slope of a solar cell with 50 mΩ series resistance near the open circuit voltage is less steep than an ideal solar cell with no series resistance as shown in Figure 4. Further increase of series resistance decreases the slope further. The slope of an IV curve with 200 mΩ series resistance is almost a straight line as shown in Figure 4.

Similarly, the major effect of shunt resistance appears on the slope of the IV curve near the short circuit current density. In case of an ideal solar cell in which there is a huge shunt resistance, the slope near the short circuit current density is very low, i.e. almost horizontal. In this case the fill factor of the solar cells is also very high.

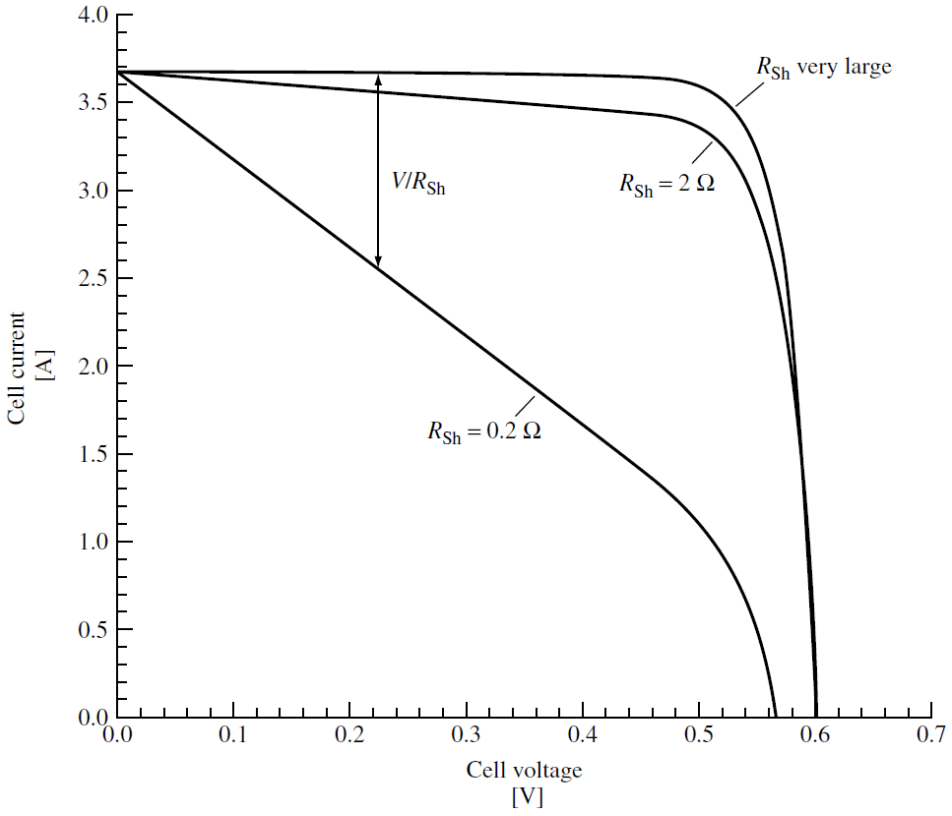

Figure 5. Effect of shunt resistance on the current-voltage curve of a solar cell. Reprinted from Luque and Hegedus (2003) [7, 11].

As the shunt resistance decreases, the slope near the short circuit current density increases accordingly. For instance, the slope of a solar cell with 2 Ω shunt resistance near the short circuit current density is steeper than an ideal solar cell with infinitely large shunt resistance as shown in Figure 5. Further decrease of shunt resistance increases the slope further. The slope of an IV curve with 0.2 Ω shunt series resistance is very steep as compared to a high quality solar cell with large shunt resistance as shown in Figure 5.

Incident photon to current conversion efficiency (IPCE) is another technique usually used to measure the quantum efficiency of the solar cells, which tells about their efficiency to convert the incident light which is a function of wavelength into electricity.

2.2 Literature review of different kinds of photovoltaic technologies

The fundamental factors which affect the commercialization of a PV technology include its performance expressed in terms of efficiency, durability and price. Other important factors include the availability of materials used and their impact on environment. PV technologies can be categorized into three different generations which are summarized in this section.

2.2.1 First generation crystalline silicon technology

The first generation of PV technology is based on crystalline silicon. Today almost 85% of the PV technology is dominated by this technology [33]. In laboratory scale, efficiencies around 27% have been obtained and around 24% have been achieved on commercial scales [8]. Theoretically maximum efficiency of a crystalline silicon solar cell cannot exceed 32%. The structure of crystalline silicon solar cells consist of a PN junction as shown in Figure 6.

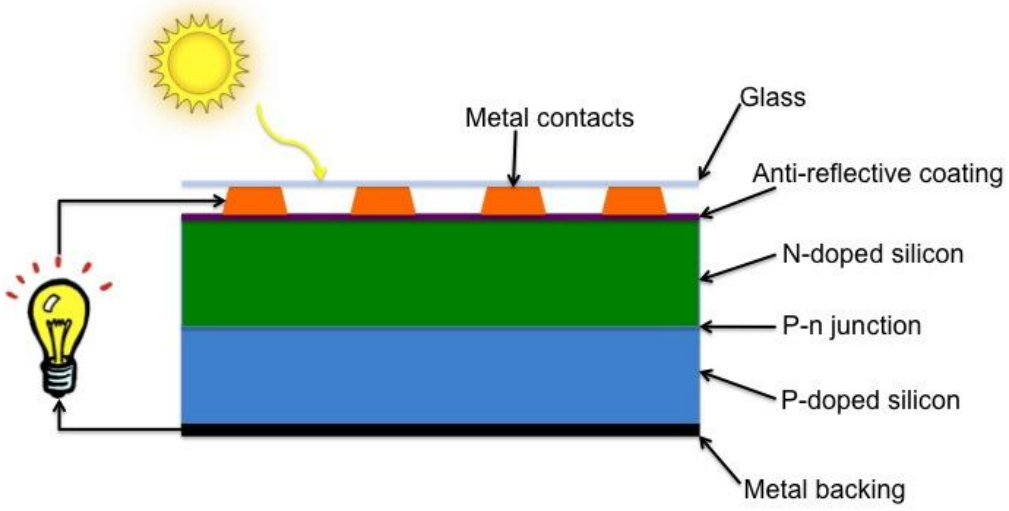

Figure 6. Structure of a crystalline silicon solar cell. Reprinted from Frompo [8].

As shown in figure 6, P side is boron doped silicon and N side is phosphorous doped silicon. Usually N side is coated with anti-reflection coating to improve the light absorption and metal contacts for current collection. Similarly P side is usually covered with metal backing to reflect the light and for completing the electric circuit. The solar cells are encapsulated with a transparent and durable glass.

The crystalline silicon PV technology can be further classified as mono-crystalline and multi-crystalline or poly-crystalline. PV modules based on mono-crystalline and multi-crystalline solar cells are shown in Figure 7. Typical module efficiencies of monocrystalline and polycrystalline are between 13-19% [10].

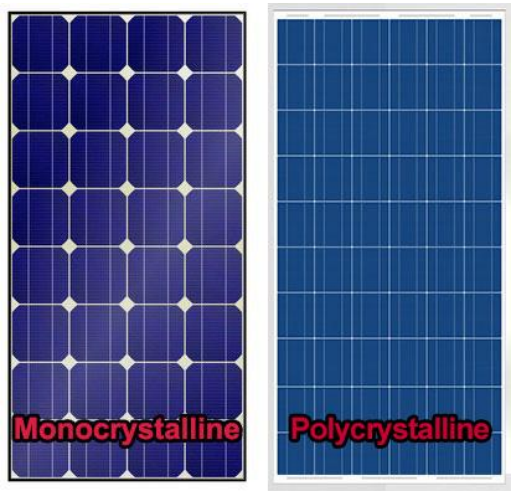

Figure 7. Typical modules based on mono-crystalline and poly crystalline silicon Technology. Reprinted from Solar Quotes [9].

Mono-crystalline solar cells are more efficient and expensive as compared to multi-crystalline silicon solar cells. The main advantage of these first generation solar cells is their long durability, i.e. over 25 years.

2.2.2 Second generation thin film photovoltaic technology

Thin film technology as the name suggests is much thinner than conventional first generation solar cells which are generally around 200 micrometer. Their thickness ranges from few nanometers to few tens of micrometers [11].

The PV technologies that fall in this category include amorphous silicon (a-Si), micro-crystalline silicon (<μ>-Si), cadmium telluride (CdTe), copper indium gallium selenide (CIGS) and gallium arsenide (GaAs). Among these technologies GaAs solar cells are the most efficient among thin film technology with an efficiency of 28.8%. Despite this high efficiency, the commercialization of GaAs solar cells is limited to only space application due to their very high costs. Recently, CIGS and CdTe solar cells have reached 21.5% and 21.7% respectively. On the other hand, the efficiency of a-Si is limited to

13.4%. Typical module efficiency is between 4%-12%. As an example, PV modules based on a-silicon, CIGS and CeTd solar cells are shown in Figure 8 [12].

Figure 8. Typical modules based on a-silicon. silicon Reprinted from Civic Solar (2010) [16], CIGS. Reprinted from Global Solar (2015) [17] and CdTe Reprinted from Phy.org (2011) [18].

In 2015, the shares of a-silicon, CIGS and CdTe in thin film PV market are about 27%, 37% and 36% respectively [13]. The main advantage of all these three technologies is to manufacture flexible PV panels unlike in the first generation of PV technologies. CIGS technology utilizes expensive and complex manufacturing methods which limits their commercialization [14]. However, they still have environmental advantage over the CdTe technology which uses a higher level of poisonous cadmium. a-silicon has very low manufacturing costs which makes it very cost competitive. However, it is not as durable as the first generation solar cells [15].

2.2.3 Third generation photovoltaic technology

Third generation PV technologies include organic solar cells, dye-sensitized solar cells, perovskite solar cells, quantum dot solar cells and multi-junction solar cells. Multi-junctions cells are the most efficient among all types of PV technologies. They have achieved 46% efficiency. However, these cells are very expensive and not suitable for terrestrial use. These cells are used for space applications. Other third generation PV technologies are low cost and suitable for large scale roll to roll production. The efficiencies obtained

by organic, dye-sensitized, perovskite and quantum dot solar cells are 11.1%, 13.4%, 20.1% and 9.9% respectively [12].

Organic solar cells utilize bulk-heterojunction to absorb the light and create charge carriers, i.e. electrons and holes. Dye sensitized solar cells consist of dye sensitized anode, redox electrolyte and cathode, sandwiched between the two conducting substrates. The light is absorbed by the photo sensitive dye which injects electrons into the conduction band of TiO_2 [23].

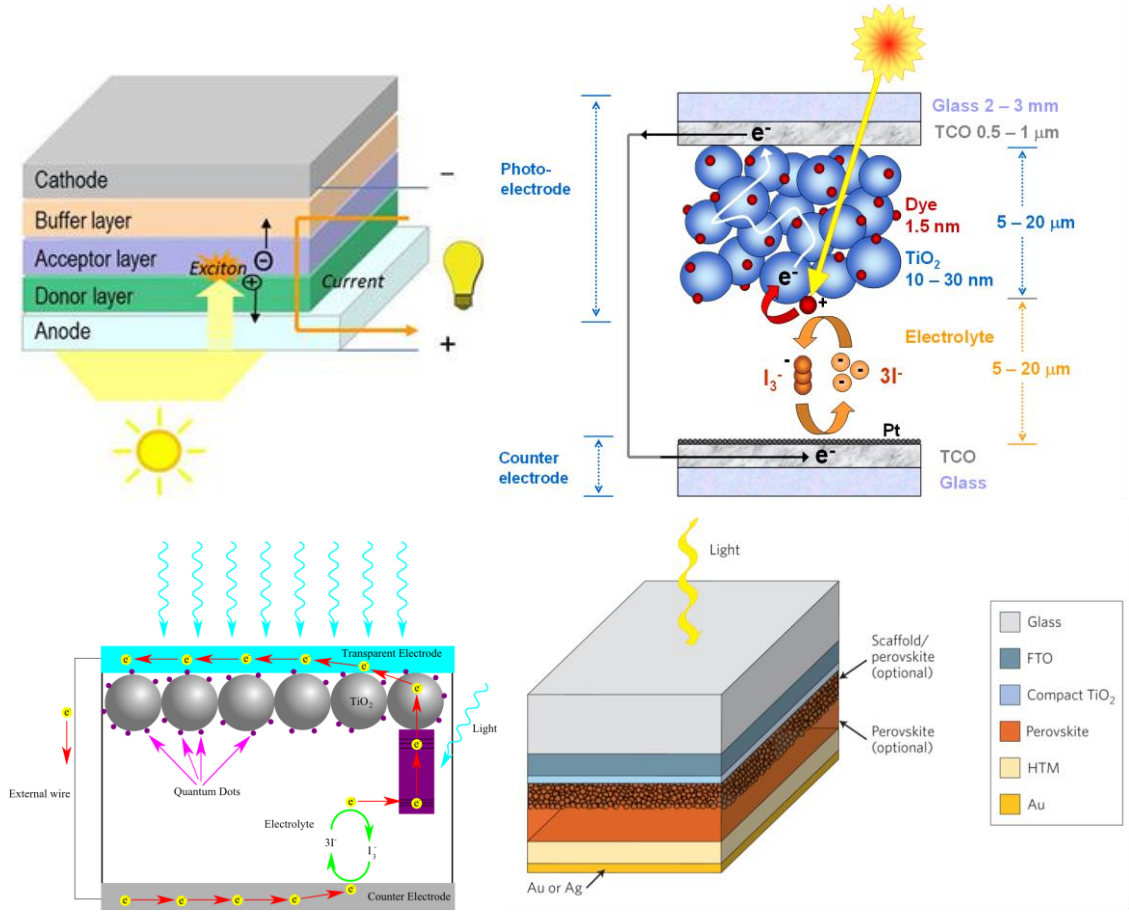

Figure 9. Structure of organic, dye-sensitized, quantum dot and perovskite solar cells [1].

The electrolyte regenerates the oxidized dye and gets reduced at the cathode. In perovskite solar cells, the perovskite material is used to absorb the light. In case of quantum dot solar cells, the light is absorbed by the quantum dots. The structure of organic, dye-sensitized, perovskite and quantum dot solar cells are shown in Figure 9.

One common element of all these solar cells is that they utilize transparent conducting oxide (TCO) substrates. The most common TCO materials are indium doped tin oxide (ITO) and fluorine doped tin oxide (FTO).

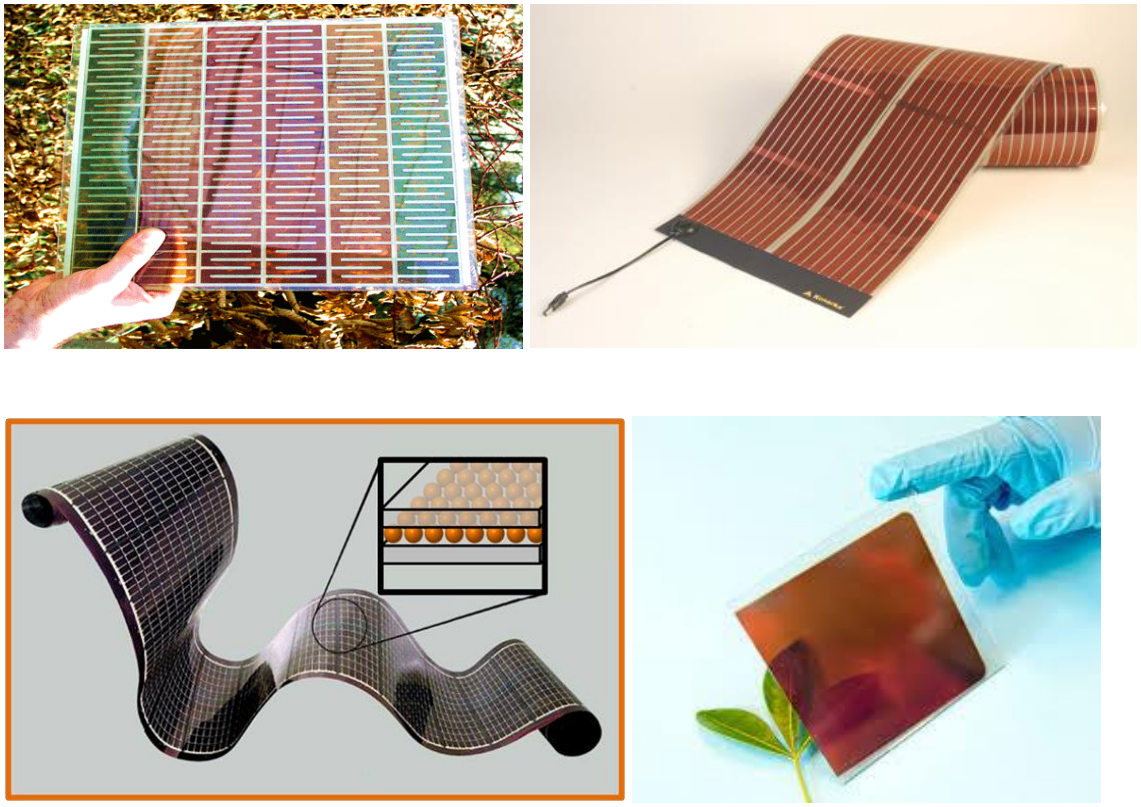

Figure 10. Modules of dye-sensitized. Reprinted from Winfried Hofmann as quoted in [24], organic. Reprinted from Konarka as quoted in [25], quantum dot. Reprinted from Masschusetts Institute of Techology [26] and perovskite solar cells.Reprinted from physics world.com [26].

Graphene and carbon nanotubes have also been used as TCO. Depending on the substrate materials, these solar cells can be either made rigid or flexible. Typical substrate materials are FTO or ITO coated glass, ITO-PET and ITO-PEN. The modules of these third generation solar cells are shown in Figure 10.

2.3 Current state of the art of printing technologies in photovoltaic applications

There are numerous types of printing technologies that have been used in various photovoltaic applications. This section will provide a brief overview of the printing technology and its corresponding use in photovoltaic technologies.

2.3.1 Screen printing

Screen printing is one of the most industrially accepted and popular printing processes. This printing method is suitable for a high rate of production. It is simple, low-cost and fast. In this method a mesh with desired printing design is used to print. Ink is placed over the mesh and the mesh is placed over the substrates on which printing is desired. The mesh is pressed with the help of a moving blade or squeegee. It results in transferring of the ink through the designed pattern to the printing surface.

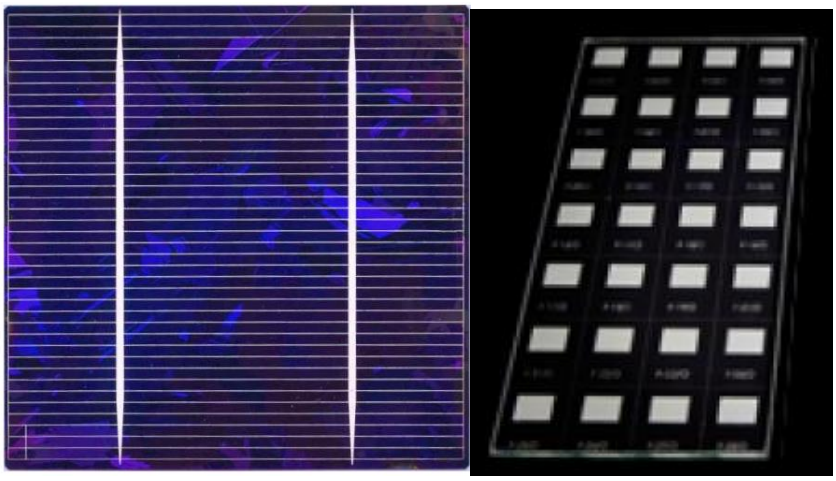

Figure 11. Screen printed silver for current collection and TiO_2 meso-porous film for dye sensitization. Reprinted from Dye Sol LTD [28].

In PV application, it is the most common method for depositing desired films because of its suitability for large scale roll to roll production. Some of the applications of screen printing include printing of silver contacts on solar cells and deposition of TiO_2 meso-porous layer in dye sensitized solar cells as shown in Figure 11.

2.3.2 Ink-jet printing

Ink-jet printing is another robust printing method which can be used to print any desired pattern as shown in Figure 12. The main advantage over screen printing is that material wastage is reduced in ink-jet printing. However, the main challenge with this printing

technique is that inks for most commonly used materials in PV technology are not developed in large scale. Ink-jet printing is mostly used for printing the electrical connections in silicon solar cells [29].

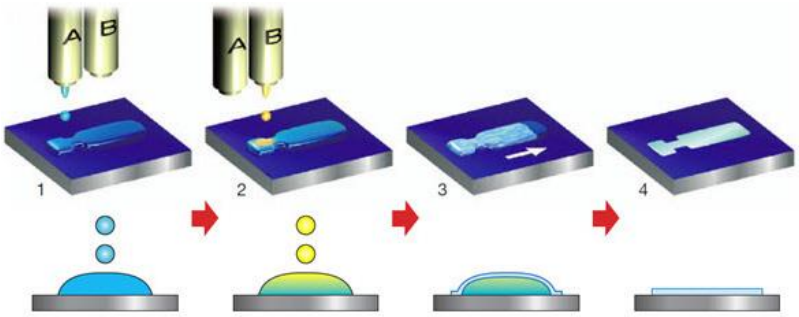

Figure 12. Inkjet printing process for manufacturing of organic thin films. Reprinted from Kazuo Takimiya as quoted in [31].

Anti-solvent ink (A) is first inkjet-printed, followed by solution ink (B) overprinted sequentially to form droplets restricted to a predefined area. Thin films grow at liquid–air interfaces of the droplet before the solvent completely evaporates. It has been used to manufacture complete CIGS solar cells [30] and organic solar cells [32]. It has also been used for depositing TiO_2 films of dye sensitized solar cells [33].

2.3.3 Laser printing

The Laser printer has been used to demonstrate the high temperature stability of paper based PV [34]. Laser printing has been used to fabricate high efficiency solar cells [35]. The main advantage is that it can replace conventional photolithography which is not compatible for the PV industry requirements.

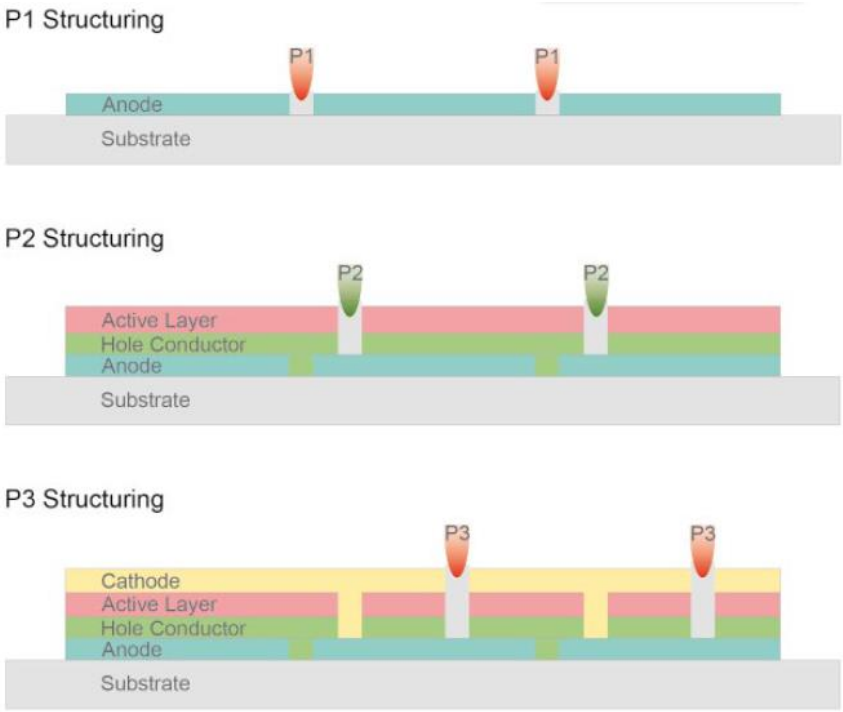

Figure 13. Laser assisted structuring of organic solar cells. Reprinted from Laser Technik Journal (2013 [36].

Organic PV cells have been manufactured using laser structuring [36] as shown in Figure 13.

2.3.4 Thermal evaporation

Thermal evaporation is a useful technique for depositing thin films. In this method the desired material is heated in a vacuum and the substrate is placed at a certain distance from the source. The evaporated materials are deposited onto the substrate as shown in the Figure 14. The thickness of the deposited film depends on the evaporation time. However, the deposited layer may not be fully uniform over a large area substrate. It is a common method in organic solar cells for depositing organic molecules in high vacuum

environment [37]. Thermal evaporation has been used to fabricate the Al and Ca layers in organic solar cells which achieved 10% efficiency [38].

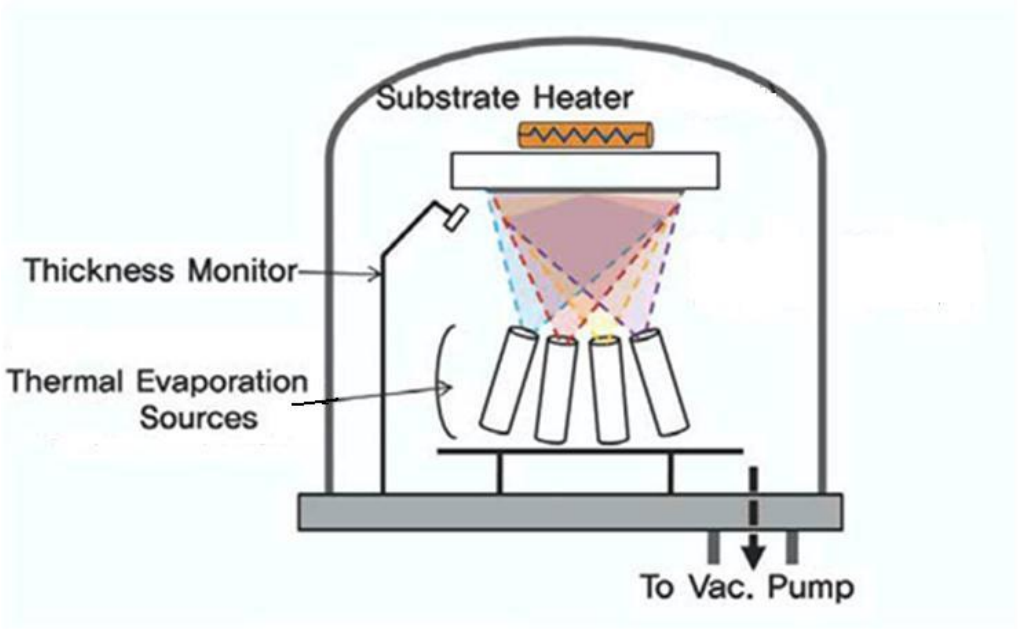

Figure 14. Co-evaporation of CIGS thin film solar cells.
Reprinted from Sne Research (2011) [46].

The perovskite absorber has been deposited by a thermal evaporation system [39]. In dye sensitized solar cells, silver electrodes have been thermally evaporated [40]. In another study Gold is deposited as a cathode using thermal evaporation in perovskite solar cells [41]. In silicon solar cells, thermal evaporation has been used to deposit Al rear side contacts [42]. Copper has been deposited using thermal evaporation in CIGS solar cells [43]. In CIGS solar cells, a CdS buffer layer has been deposited using chemical bath deposition (CBD), thermal evaporation, sputtering, atomic layer deposition, and spray ion layer gas reaction. The “dry” deposition methods like sputtering and thermal evaporation could be favorable in an industrial environment on glass substrates or application in a roll to roll coater [44]. In other studies, CdTe solar cells were entirely fabricated with thermal evaporation [45].

2.3.5 Sputtering

In the sputtering method the atoms of a solid target material are ejected due to bombardment by highly energetic particles. These ejected particles are deposited onto the sub-

strate placed under the target material as shown in Figure 15. It is very useful in depositing thin films with thicknesses varying from a few nanometers up to tens of micrometers. There are several types of sputtering including DC sputtering, RF sputtering and magnetron sputtering. Magnetron sputtering is the most commonly used due to a higher sputtering rate. The main advantage of sputtering over the evaporation technique is that better adhesion of the films onto the substrate is obtained using sputtering method.

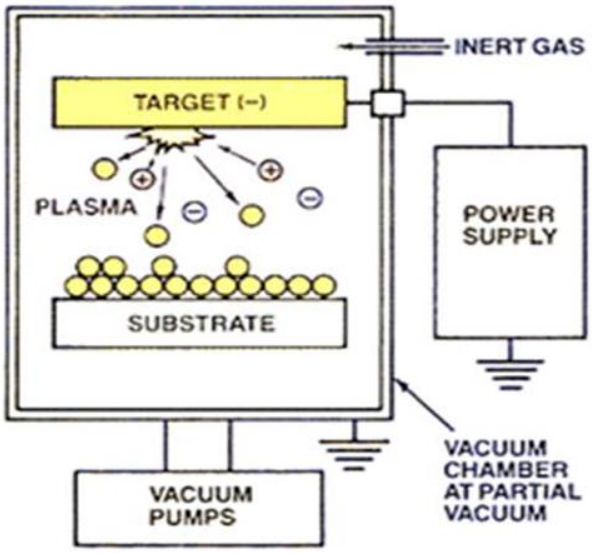

Figure 15. Sputtering process for depositing thin films. Reprinted from Sne Research (2011) [46].

Sputtering has been widely used to manufacture high efficiency CdTe solar cells [47] and an efficiency of 14% has been achieved by all sputtered CdS/CdTe solar cells [48]. An efficiency of around 8% has been obtained for CIGS solar cells employing the sputtering process [49].

Sputtering of amorphous silicon onto crystalline silicon has been reported to form heterojunction solar cells [50]. In dye-sensitized solar cells, sputtering of platinum onto the stainless steel metal substrates has been reported to stabilize the solar cells [51].

2.3.6 Spin coating

It is a method to deposit thin films of uniform thickness on a flat substrate. In most common configuration, the material is applied onto the substrate. Then the substrate is set for rotating with a certain speed for a certain time. The material on the substrate is spread due to centrifugal force. Afterwards, the film is dried before depositing any further film material. The process is shown in Figure 16.

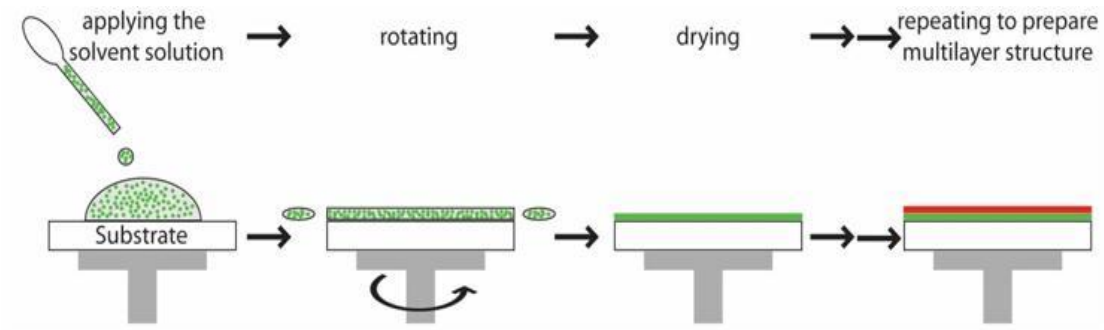

Figure 16. Spin coating process for depositing thin films.
Reprinted from Sne Research (2011) [46].

In organic solar cells, a PEDOT:PSS layer is often spin coated [52]. Other organic materials such as photosensitive layers have been spun coated [53]. In CIGS solar cells, antireflection coating has been reported to be deposited by spin coating [54]. In other studies, nanocrystals of CdTe were deposited using the layer by layer spin coating process; however, the efficiency was limited to only 2 % [55]. In dye sensitized solar cells, spin coated TiO_2 films have been deposited to improve the stability of the solar cells [56]

2.3.7 Chemical vapor deposition and electrochemical deposition

Chemical vapor deposition (CVD) is frequently used in various industries to deposit thin film. In its simplest configuration, precursor gases are flown into a controlled chamber where one or more heated objects to be coated are placed [57] as shown in Figure 17. The deposited film can be amorphous, mono-crystalline or poly-crystalline depending on the material properties and the conditions (temperature, pressure) set in the chamber.

Thin film of silicon (10-50 µm) has been deposited using CVD at the high temperature of 1100^{o}C to achieve a 17.6% efficient silicon thin film solar cell [58]. Around 4.3% efficient

flexible organic solar cells have been fabricated using a CVD grown graphene electrodes [59]. In another study, large area CVD grown graphene were used as transparent electrode for efficient organic solar cells [60]. The metal organic chemical vapor deposition (MOCVD) method has been employed to fabricate CdTe and CIGS solar cells [61]. For dye sensitized solar cells, CVD grown TiO_2 particles were used for light scattering for improving the light absorption which improved the performance up to 22% (from 4.4% to 5.4% efficiency) [63.]

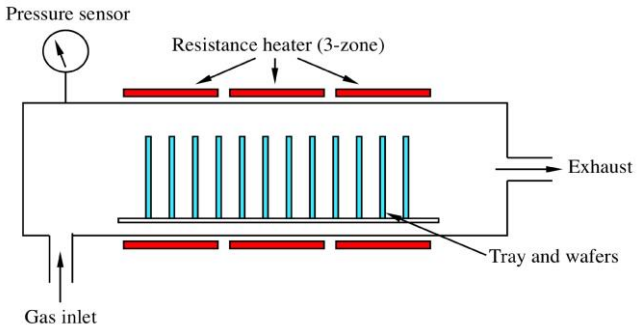

Figure 17. Chemical vapor deposition process.
Reprinted from Rice University (2015) [64].

Like CVD, electrochemical deposition has been used for manufacturing of different kinds of PV technologies such as dye sensitized [61] and CdTe solar cells [62].

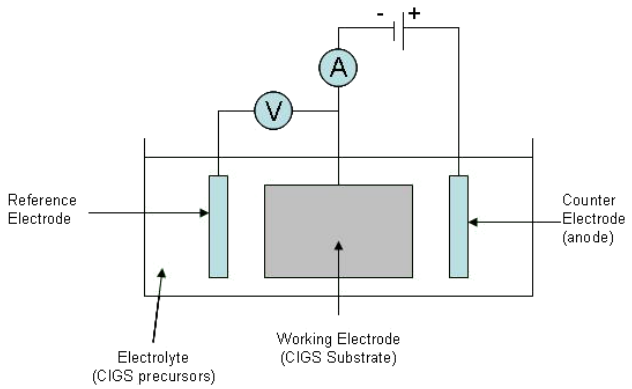

Figure 18. Electrochemical deposition for CIGS manufacturing
Reprinted from Sne Research (2011) [46].

The process of electrochemical deposition for CIGS thin film solar cells is presented in Figure 18.

2.3.8 Photolithography and Nano imprinting

Photolithography is also known as optical as lithography or UV lithography. It is used to pattern a thin film or the bulk of a substrate. In photolithography, the first step is to clean the wafer to remove any organic, ionic and metallic impurities. Afterwards a barrier layer on the top of wafer is deposited. Then a photoresist is applied on the barrier layer usually using the spin coating method. The structure is basked to remove solvents from the photoresist coating.

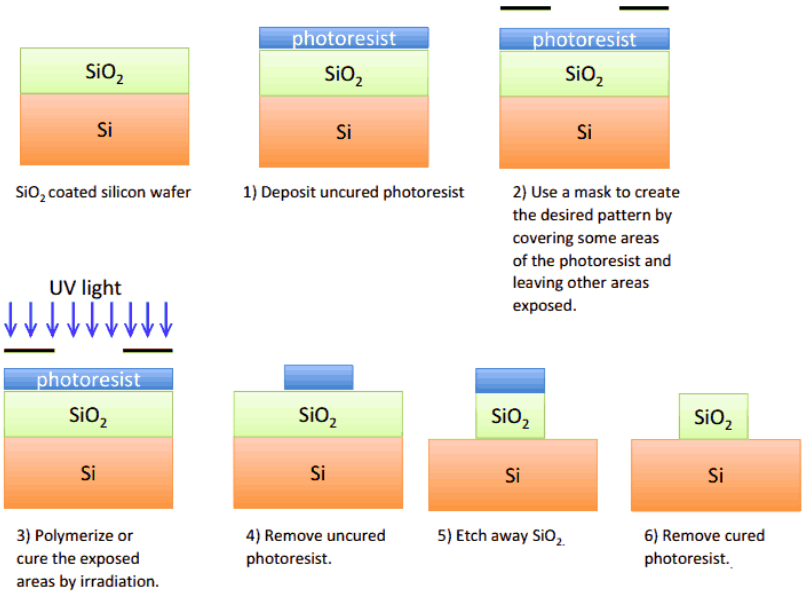

Figure 19. Chemical vapor deposition process. Reprinted from MRSEC Education Group (2015) [66].

A photomask with the desired pattern is placed and aligned with the wafer. Then it is exposed to UV illumination. The part of the photoresist gets exposed to UV light through the pattern on the photomask. There are basically two kinds of photoresists, i.e. positive photoresist and negative photoresist. Positive photoresist change chemical structure upon UV exposure in such a way that the structure becomes more soluble in the developer. Negative photoresist change chemical structure upon UV exposure in such a way that the structure becomes more insoluble in the developer. The structures are then exposed to a developing solution from in which a photoresist is removed according to the pattern on the photomask. Finally, the resulting structure is hard-baked to harden the

photoresist and to improve its adhesion on the wafer surface [65]. The lithography process is shown in Figure 19.

Photolithography is a common method to form contacts in crystalline silicon solar cells as it is suitable for large scale mass production. The highest efficiency crystalline silicon solar cells have used this method for their fabrications as well. [67]. There are several limitations to the use of the lithography method. For instance, it requires an expensive facility, a number of process steps and slow speed [68].

In thin film solar cell manufacturing, imperfect patterning due to errors in alignment steps in lithography results in decrease in the performance of the cells. It has been observed that on a laboratory scale where photolithography is implemented more carefully, the CIGS solar cells resulted in around 20.3% efficiency. However, the CIGS solar cells were around 10-14% when manufactured in mass production [68].

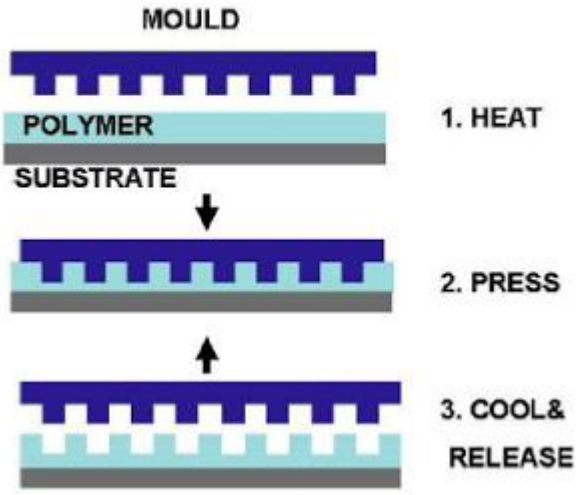

Figure 20. Nanoimprinting process: Mould is applied on the resist by imprinting (1). The pressure is maintained (2). The mold and substrate are cooled and separated. Reprinted from Brian Wang (2011) [69].

Nanoimprinting or nano imprint lithography is a novel method for fabricating nanometer scale patterns. It has low cost, high throughput and high resolution. The main difference between Nanoimprinting and photolithography is that in photolithography photos or electrons are used to modify the chemical and physical properties of the photoresist, whereas in Nanoimprinting the resist is deformed mechanically as shown in Figure 20. Nanoimprinting offers a better resolution than photolithography because unlike photolithography

it is not affected by light diffraction or beam scattering [70]. Nano imprinting has been effectively used in crystalline silicon [71], thin film [72] and third generation solar cells [73; 74].

2.3.9 Electrophotography

The working principle of electrophotography which is also known as xerography is based on electrostatic charges. It is a printing and photocopying method that uses electricity to produce an image on a photoconductive surface [75] as shown in Figure 21.

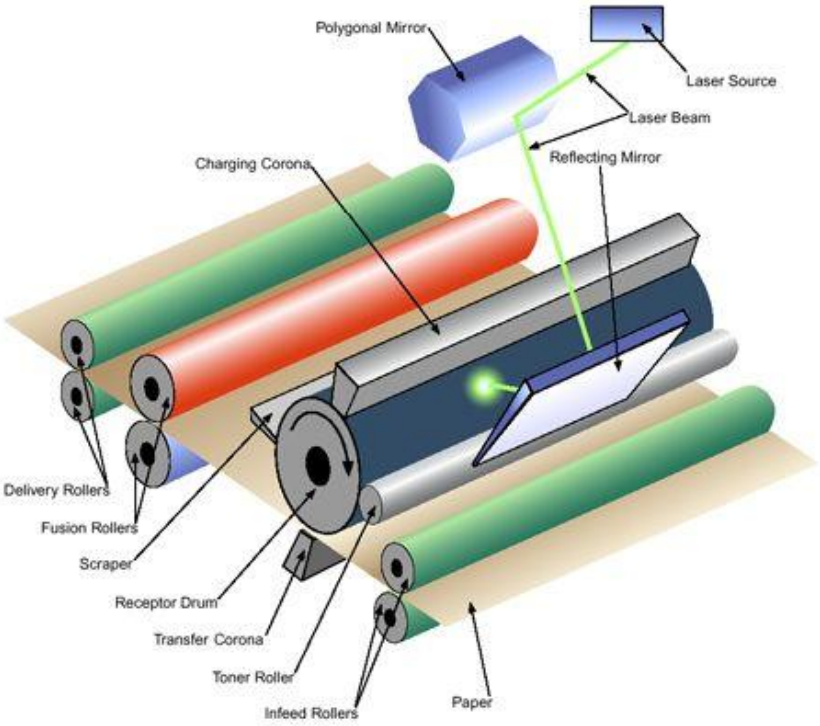

Figure 21. Electrophotography process.
Reprinted from Glossary of Printing Terms [75].

This technique is rarely used in PV cell manufacturing. There is a patent in which some organic dyes are reported to both photovoltaic cells and photoconductive electrophotography systems [76].

2.3.10 Lamination technology

Lamination in broad terms is a process of building up successive layers of a substance and bonding them together using adhesives. Primarily, there are three kinds of lamination machines. One type uses pouches, the second uses film and the third uses UV liquid for coating the print. Among them, UV liquid laminators are the most complex ones. They are expensive and hard to operate, requiring power consumption and ventilation [77]. The main purpose of lamination is to protect print, film or any other substance. Figure 22 shows a typical vacuum lamination machine and a roll lamination machine.

Figure 22. Vacuum lamination machine. Reprinted from Xinology Co, Ltd [91] and roll lamination machine Reprinted from Bright Stationary Co,Ltd (2010) [92].

Generally, PV modules are encapsulated using a vacuum lamination machine. The vacuum lamination machine is expensive and slow in process. It usually takes 8-20 minutes for glass/back sheet and 8-25 minutes for glass/glass modules [78]. Recently, encapsulation of PV cells using a roll lamination machine has been reported. The roll lamination is significantly cheaper and faster than vacuum lamination. It takes approximately 1 minute to encapsulate a PV module [78].

2.3.11 Sheet-fed and web printing

Sheet-fed press prints on individual sheets of papers unlike web presses where printing is done on continuous roll of paper [79]. Web presses can print both sides of the sheet in one pass, whereas conventional sheet-fed presses can print each side separately [80]. Typical sheet-fed and web printing machines are shown in Figure 23.

Figure 23. Sheet-fed printing. Reprinted from Qingdao 2FC Trading (2015) [85] and Web printing. Reprinted from Baldwin Technology group (2004-2014) [90].

Sheet-fed press has excellent job flexibility. It is cheaper than the web press and suitable for large formats such as large posters, special colors, unusual sizes and heavy gloss papers. On the other hand, the web press is much faster than the sheet-fed and runs efficiently in long-term operation. Furthermore, it suits more standard jobs such as printing brochures, newspapers and magazines [81]. Both of these technologies have been used for manufacturing of organic solar cells [82; 83; 84].

2.3.12 Gravure

Gravure is a printing technique, which utilizes engraved cylinders or cylinder-mounted plates as the image carrier [86]. In this printing method an image is etched on the surface of a metal plate or cylinder [87] as shown in Figure 24.

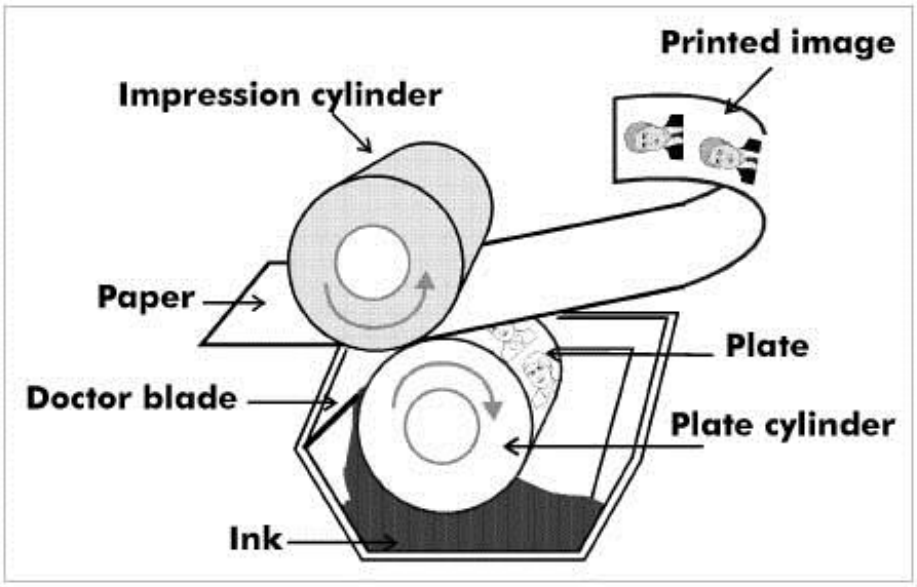

Figure 24. Gravure printing. Reprinted from Illinois Sustainable Technology Center (2015) [89].

Most gravure printing performed today is web-fed rotogravure printing, with occasional sheet-fed use. Gravure is also well suited to the printing of packaging on a variety of non-paper substrates [86]. This printing method has been used in the manufacturing of organic solar cells [88].

2.3.13 3D printing

3-dimensional (3D) printing is a process of forming 3D solid objects from a digital image. The creation of a 3D object is realized by using additive processes. In an additive process, successive layers of materials are laid down to create a 3D object [93]. 3D printing is also known as additive manufacturing. Usually an automated printer follows a digital design to create a 3D print by repeatedly laying down materials like glass, silicon, plastic,

resin and ceramic materials on top of each other until the final 3D printed object is completed [94]. A typical 3D printer is shown in Figure 25.

Figure 25. 3D printer. Reprinted from Amazon (2015 [99] and 3D printed solar trees for light harvesting. Reprinted from VTT Technical Research Center [100].

As the 3D printing works on a digital design instead of a conventional assembly line for PV manufacturing, it can save huge shipping costs as the PV panels can be created anywhere with the help of 3D printer [94]. There has been a lot of research conducted on using printing for organic PV manufacturing [95; 96] and novel printed designs are presented for solar light harvesting such as 3D printed solar energy trees [97]. Interestingly according to Japan Aerospace Exploration Agency (JAXA), it is possible to transmit 1.8 kilowatts of solar generated power using microwaves to a receiver around 180 feet from the power source and in conjunction with 3D printing, it would allow to drive vehicles or factories in space in the future [98]. Thin and flexible 3D printed solar cells are made from materials such as cloth. These lightweight solar cells are under tests for different applications including rooftops, vehicles and other power electrical systems [98].

3 Experimental section

In this section, experimental details of three different types of solar cells' manufacturing and their corresponding measurement setups are described.

3.1 Manufacturing of crystalline silicon solar cell

In these experiments, already made multi-crystalline silicon solar cells were used. The electrical connections of the solar cells were made with the help of soldering equipment. For this purpose, silver wires were used which were coated with lead to help the soldering process. After establishing the electrical contacts, the solar cells were placed over the laminate material. Then the top side of the solar cells was also covered by another sheet of laminate materials. The laminate materials were polyester films coated with EVA. The laminate material over the electrical contact near the edges was removed and finally the solar cells covered by laminates from both sides were fed into the roll laminator. The lamination speed was set to 10 RPM and the rollers temperature was set to 150^{o}C. With these settings, the solar cells were encapsulated with the help of roll a lamination machine. The laminated solar cells were then bonded onto a structural board with the help of glue. A photograph of the prototype crystalline silicon solar cells manufactured in this project can be seen in the Appendix 2.

3.2 Manufacturing of organic solar cell

Due to limited resources, ready-made organic solar cells were used in this project for measurements. The organic solar cells were based on PEDOT: PSS and PCMB: P3HT on ITO coated glass. Electrical contacts were made using adhesive copper tape. Finally silver paste was applied on the contacts to improve the adhesion which would decrease the contact resistance. The silver ink took some time to dry. Then the solar cells were ready for measurements.

3.3 Manufacturing of dye-sensitized solar cell

In this project, dye-sensitized solar cells were manufactured using the screen printing method. First, FTO coated 2 mm thick glasses were cut into small pieces of the size 16 mm x 20 mm. A pair of holes was drilled on to some of these substrates. Then these substrates were washed using detergent in an ultrasonic bath. The substrates were further washed with ethanol and acetone. Then they were dried in an oven.

The photo-electrodes of the solar cells was prepared by screen printing a meso-porous layer of TiO_2 of the size 4 mm x 8 mm onto the clean FTO coated glass substrates. The layers were heated at 110^{o}C for 30 minutes, then cooled to room temperature. Then another layer of TiO_2 was applied using same procedure. The reason to deposit two layers was to get the total thickness of the TiO_2 layer around 10 µm. The thickness of the film was measured using a profilometer. The photo-electrodes were then placed in a dye solution consisting of 0.32 mM of the N719 dye in ethanol (99.5 wt %) for sensitization. They remained in the dye solution for about 24 hours. After that the photo-electrodes were ready for cell assembly. The counter-electrodes were prepared by depositing approximately 5 nm (thick) layer of platinum on clean FTO coated glass substrates by the sputtering method.

An approximately 25 µm thick Surlyn foil with 5 mm x 14 mm aperture was placed on the top of the sensitized photo-electrode. Then the counter-electrode substrate was placed on the top of the foil in such a way that the platinum layer and the sensitized layer were facing each other. The assembly was placed on a hot place set at 110^{o}C. That made the two electrodes bonded with each other with a gap of approximately 25 µm. Then the electrolyte was poured in the cell through the hole. The surface was cleaned and then another Surlyn foil with the size of the substrate was placed on top of the substrate so that the holes were covered by the foil. Then thin microscopic glass was placed on top of the covering foil. Then finally the assembly was pressed at 110^{o}C for 10 seconds. Then the electrical contacts at the electrodes were made using adhesive copper tape. Silver ink was applied on the contacts between the copper tape and the FTO coated glasses. Finally to strengthen the contacts glue was applied on the contacts which were left to dry for a few hours. Then the dye-sensitized solar cells were ready for measurements. A photograph of a prototype dye-sensitized solar cell manufactured in this project is attached in Appendix 2.

3.4 Measurements of solar cells

The performance of the solar cells was measured using solar simulator at New Energy technologies Group at Aalto University. The Figure 26 shows the solar simulator and the equipment used for measuring the efficiencies of the solar cells. The main components of the solar simulator include the halogen lamps, power sources for the lamps, potentiostat, data logging machine, Peltier element for cooling, temperature sensors, light monitoring device and calibration cell.

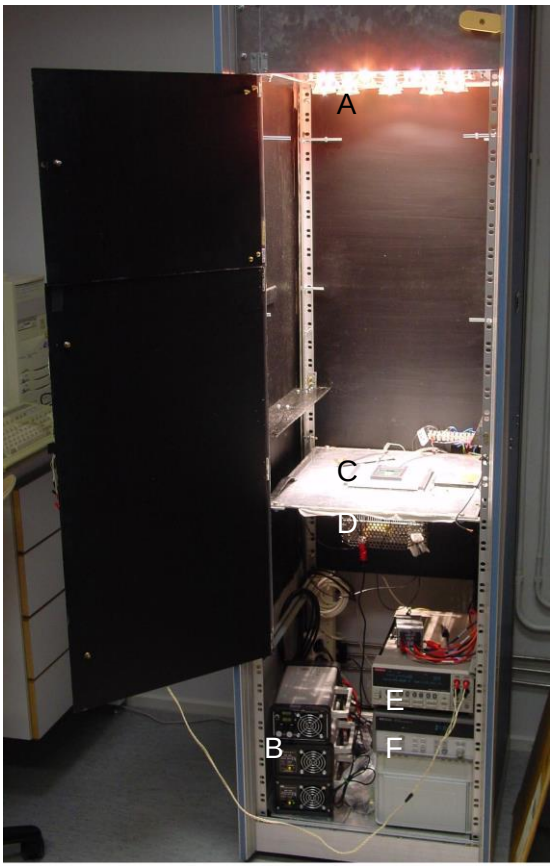

Figure 26. The solar simulator at the New Energy Technologies Group at Aalto University.

The list of components used in the solar simulator are listed below marked in Figure 26 and 27.

A) (The) simulator halogen lamps
B) Lamp power supply
C) Peltier elements for cooling the platform
D) Measurement platform
E) Keithley 2400 Source-Measure Unit (Potentiostat)
F) HP 34,970 A datalogger
G) (A) calibrated reference cell
H) Monitoring cell
I) Temperature sensor

The calibration cell, light monitoring cell and thermal sensors can be more clearly seen in Figure 27.

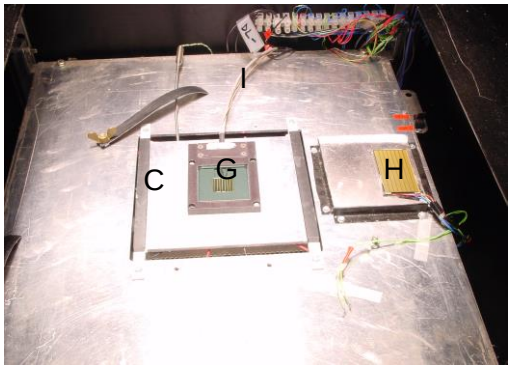

Figure 27. The calibration cell (G), light monitoring cell (H) and temperature sensor (I) in the solar simulator.

First the lamps of the solar simulators were turned on and there was a 15 minutes pause before starting the measurements. The calibration cell was placed in the center of the solar simulator and the light intensities were calibrated for 1 Sun light intensity, i.e. 1000 W/m^2.

The monitoring cell was continuously measuring the light intensity after every second to make sure that the light intensity did not change during the measurements. Then the I-V curves of the solar cells were measured one by one at room temperature using Keithley 2400 Source-Measure Unit (Potentiostat). The Measurement equipment was controlled

by the Agilent VEE Pro software programme. A screenshot of the software is attached in Appendix 3.

The I-V data was recorded and saved as a text file. Then the efficiencies of the solar cells were calculated using Eq. 5. The Matlab code used for this purpose is attached in Appendix 1.

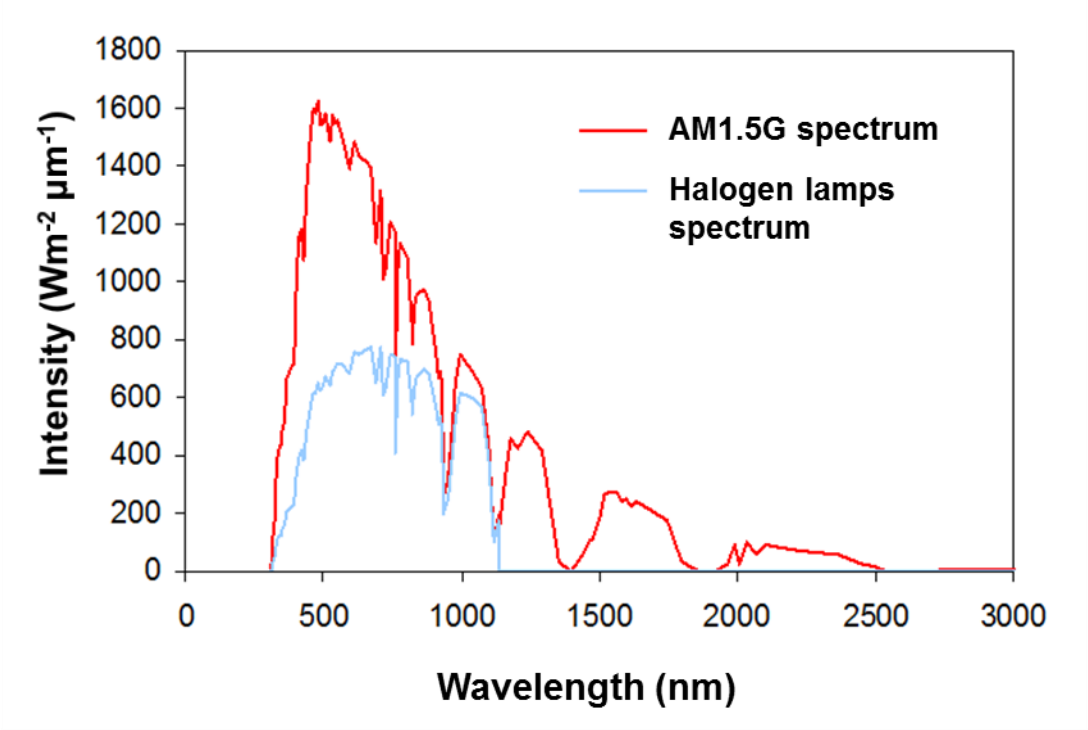

Figure 28. The spectrum of sunlight and halogen lamps.

Since the spectrum of the halogen lamps is different from the actual sunlight as shown in Figure 25, spectral mismatch is taken into account in the calculations by multiplying the current density values by a factor of 0.94.

4 Results and discussion

In this section, the measurement results of the three different types of solar cells are presented and analyzed. The efficiencies of the solar cells were obtained by measuring the current-voltage curves of the solar cells under 1 Sun equivalent light intensity, i.e. 1000 W/m^2 at room temperature. The performance limiting factors are briefly discussed as well.

4.1 Measurements of a crystalline silicon solar cells under 1 Sun lighting condition

The current-voltage and power-voltage curves of the crystalline silicon solar cells are shown in Figure 29. It seems from the slope of the IV curve near the open circuit voltage that the crystalline solar cell has quite high series resistance. The effect of the series and shunt resistance on the IV curve are shown in detail in Figure 3 and 4. The IV curve of the crystalline solar cell seems to have adequate shunt resistance.

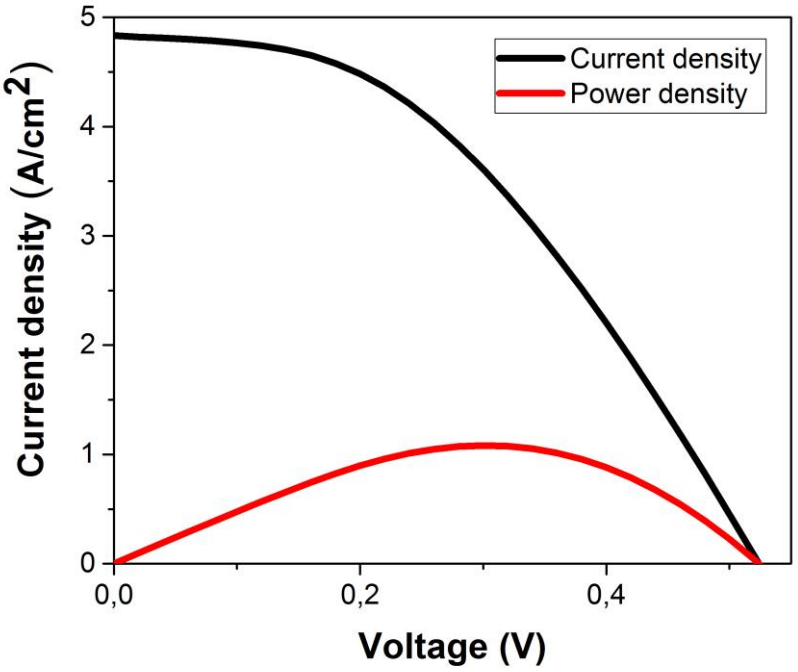

Figure 29. The current-voltage and power-voltage curves of the crystalline silicon solar cell measured under 1 Sun equivalent lighting conditions.

The performance parameters including open circuit voltage, short-circuit-current-density and fill factors are calculated using Eq. 5 and are presented in Table 1.

Table 1. The performance parameters of the multi-crystalline silicon solar cell.

Crystalline silicon solar cell	**Values**
Short circuit current density (A/cm^2)	4.8
Open circuit voltage (V)	0.52
Fill factor (%)	0.58
Efficiency (%)	14.5

The values resulted in a solar cell efficiency of 14.5%. The solar cell efficiency would have been 21% if the fill factor would have been 85%. However, primarily due to high series resistance and to some extent due to recombination, the efficiency of the solar cell is limited to 14.5%.

4.2 Measurements of organic solar cell under 1 Sun lighting condition

The current-voltage and power-voltage curves of the organic solar cell are shown in the Figure 30. It seems from the slope of the IV curve near the shortcircuit current density point that the organic solar cell has quite high shunt resistance which effectively blocked the leakage currents. Furthermore, the series resistance is also not very high. The re-combination also does not have much effect on the IV curve.

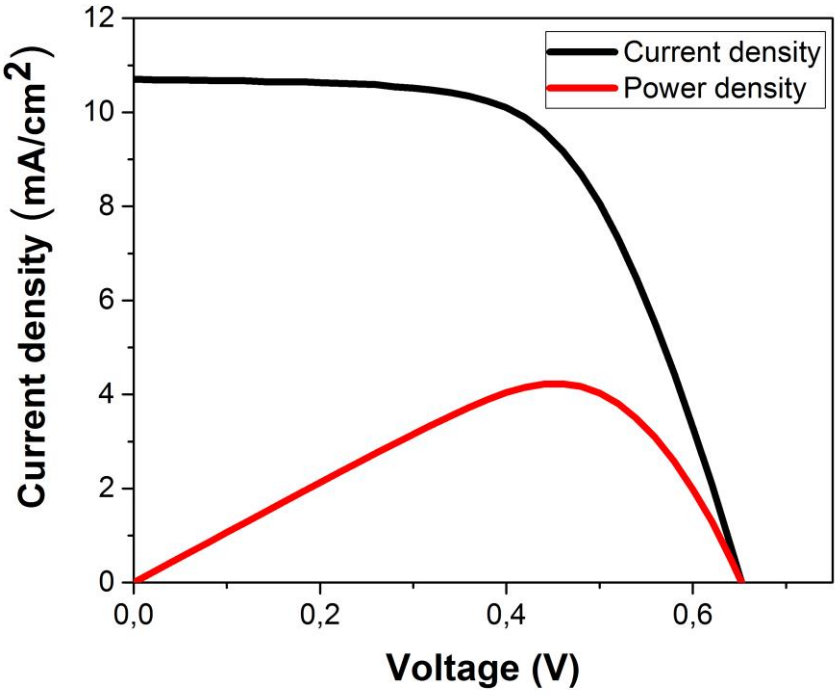

Figure 30. The current-voltage and power-voltage curves of the organic solar cell measured under 1 Sun equivalent lighting condition.

It seems from the slope of the IV curve near the short- circuit current density point, that the organic solar cell has quite high shunt resistance which effectively blocks the leakage currents. Furthermore the series resistance is also not very high. The recombination also does not have much effect on the IV curve.

The values of the performance parameters including open circuit voltage, short-circuit-current-density and fill factors were calculated using Eq. 5 and are presented in Table 2. The values resulted in a solar cell efficiency of 4.21%. The solar cell efficiency is primarily limited by the smaller value of short-circuit current density. The open circuit voltage is reasonably high, i.e. 0.65V. However, the fill factor can be improved by further improving the electrical contacts.

Table 2. The performance parameters of the organic solar cell.

Organic solar cell	**Values**
Short circuit current density (mA/cm^2)	10.7
Open circuit voltage (V)	0.65
Fill factor (%)	60.5
Efficiency (%)	4.21

4.3 Measurements of dye-sensitized solar cell under 1 Sun lighting condition

The current-voltage and power-voltage curves of the dye-sensitized solar cell are shown in Figure 31. It seems from the slope of the IV curve near the open circuit voltage that the crystalline solar cell has slightly higher series resistance than the organic solar cell. However, both the cells have very high shunt resistance as the slope of the IV curve near the short-circuit current density is almost zero. As a reference, the effects of series and the shunt resistances on the IV curve are shown in detail Figure 4 and 5.

Like in the organic solar cells, the IV curve of the dye-sensitized solar cell seems not to be much effected by recombination.

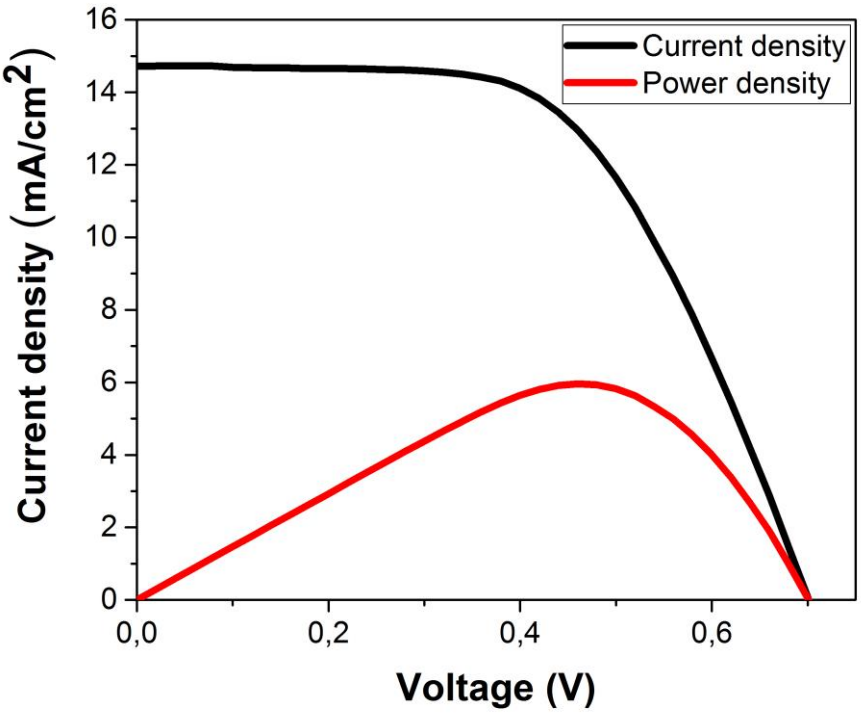

Figure 31. The current-voltage and power-voltage curves of the dye sensitized solar cell measured under 1 Sun equivalent lighting condition.

The dye-sensitized solar cell IV curve leads to slightly higher efficiency of the solar cell as compared to the organic solar cell primarily due to improved light absorption and higher open circuit voltage. Although the fill factor is slightly lower for the organic solar cell, i.e. 57.8%, as compared to organic solar cell 60.5%, the effect of short-circuit current density and open circuit voltage is dominating the overall performance of the dye-sensitized solar cell.

The values of the performance parameters including open circuit voltage, short-circuit-current-density and fill factors are calculated using Eq. 5 and are presented in Table 3. The values resulted in a solar cell efficiency of 5.94%.

Table 3. The performance parameters of the dye-sensitized solar cell.

Dye sensitized solar cell	**Values**
Short circuit current density (mA/cm^2)	14.7
Open circuit voltage (V)	0.70
Fill factor (%)	57.8
Efficiency (%)	5.94

The solar cell efficiency is primarily limited by the smaller value of short-circuit current density, though it is significantly higher than the short-circuit current density value of the organic solar cell. The open circuit voltage is quite high, i.e. 0.65V. However, the fill factor can be improved by further improving the electrical contacts.

5 Conclusions

The experimental work performed in the project describes clearly that crystalline silicon, organic and dye-sensitized solar cells, which employ numerous, printing technologies, are functioning well. Quite high efficiencies of the crystalline, organic and dye-sensitized solar cells were obtained in this project. It was noticed that the performance of some of the solar cells, which suffered due to contact resistance, can be improved by improving the current collection contacts. Printable conductive inks can be used to replace the adhesive copper tape to decrease the contact losses and hence improve the efficiency of the solar cells.

The recent developments in the printing technologies have tremendous impact on the emerging photovoltaic technology. Many of the manufacturing challenges are solved by the development of new printable materials and the easy to up-scale methods of printing. Significant improvement in photovoltaic cell performance is achieved with the help of development in printing technologies. In addition, these simple and low cost printing technologies enable decreasing the costs of the photovoltaic technologies and make them a competitive alternative to the current sources of electricity. Interestingly, all the three generations of solar cells have benefited from the versatile printing technologies. Most importantly, recent advancements clearly indicate that organic, dye-sensitized and perovskite solar cells, which belong to new emerging photovoltaic technologies, are compatible with fully printable solar cell technology. The robust printing of these vibrant technologies is revolutionizing the world. Features such as a variety of colors, flexibility and lightweight are adding additional value in the PV technology which make solar cells attractive for the customers not only because of their performance only but also due to their esthetic value.

References

1. Asghar MI. Stability issues of dye solar cells [online]. Aalto University, May 2012. Doctoral Thesis
   URL: http://lib.tkk.fi/Diss/2012/isbn9789526046112/. Accessed: 20 April 2015.

2. Pandey C, Asghar MI, Klemetti A. Recent Business Trend of Photovoltaic Technology in South Asia [online]. 29th European Photovoltaic Solar Energy Conference and Exhibition 2014; 4065 – 4068.
   URL:http://www.eupvsec-proceedings.com/proceedings?paper=31176. Accessed: 20 April 2015.

3. Eu Pvsec conference. Amsterdam, September 2014.
   URL: http://www.eupvsec-proceedings.com. Accessed 20 April 2015.

4. Lian R. Top 10 PV module suppliers in 2012 [online]. Pvtech; 2012.
   URL:http://www.pvtech.org/guest_blog/
   top_10_pv_module_suppliers_in_2012. Accessed 20 April 2015.

5. Honsberg C, Bowden S. Air Mass [online]. Pv Education.org.
   URL: http://www.pveducation.org/pvcdrom/properties-of-sunlight/
   air-mass.
   Accessed: 20 April 2015.

6. Honsberg C, Bowden S. Series Resistance [online]. Pv Education.org
   URL: http://pveducation.org/pvcdrom/solar-cell-operation/
   series-resistance.
   Accessed: 20 April 2015.

7. Honsberg C, Bowden S. Shunt Resistance [online]. PV Education.oRG.
   URL: http://pveducation.org/pvcdrom/solar-cell-operation/
   shunt-resistance.
   Accessed: 20 April 2015.

8. Frompo. Schematic of the basic structure of a silicon solar cell [online].
   URL: http://images.frompo.com/802fa49df256ac9f658aa49dc8164183.
   Accessed: 20 April 2015.

9. Peacock Media Group. Monocrystalline vs Polycrystalline Solar Panels [online]. Solar Quotes, Australia.
   URL: https://www.solarquotes.com.au/panels/photovoltaic/
   monocrystalline-vs-polycrystalline. Accessed: 20 April 2015.

10. Bas L. Thin Film vs. Crystalline Silicon PV Modules [online]. San Francisco, California: CivicSolar, Inc; 2010.
    URL:http://www.civicsolar.com/resource/
    thin-film-vs-crystalline-silicon-pv-modules Accessed: 20 April 2015.

11. Luque A, Hegedus S, editor. Handbook of Photovoltaic Science and Engineering. Chichester,West Sussex. John Wiley & Sons Inc; 2003

12. National Renewable Energy Laboratory (NREL). Research Cell Efficiencies Record [online]. National Center for Photovoltaics, The United States: Department of Energy; 2015.
URL: http://www.nrel.gov/ncpv/images/efficiency_chart.jpg. Accessed: 20 April 2015.

13. CGIS to Emerge As Major Technology [online]. Saral Gyan Capital Services. Madhya Pradesh: 2010.
URL: http://www.saralgyan.in/2010/10/
cigs-to-emerge-as-major-technology- by.html. Accessed: 20 April 2015.

14. Sale of CIGS Solar Cell Panels Expected to Reach $1 Billion by 2013. Solar Fact and Advice [online]. Delaware, US. Alchemie Limited Inc; 2013.
URL: http://www.solar-facts-and-advice.com/CIGS-solar-cell.html. Accessed: 20 April 2015.

15. What Is Amorphous Silicon? Why is it so Interesting Now? [online]. Delaware US. Alchemie Limited Inc; 2013.
URL:http://www.solar-facts-and-advice.com/amorphous-silicon.html. Accessed: 20 April 2015.

16. UniSolar PVL-144 Laminate, Amorphous, 24V Solar Panel [online]. San Francisco, California: CivicSolar, Inc; 2010.
URL:http://www.civicsolar.com/product/
unisolar-pvl-144-laminate-amorphous- 24v-solar-panel. Accessed: 20 April 2015.

17. Thin-film CIGS photovoltaic module / flexible PowerFLEX™ 6 [online]. Marseille – France: Global Solar; 2015.
URL:http://www.directindustry.com/prod/global-solar/
thin-film-cigs-photovoltaic/ module-flexible-20893-48237.html. Accessed: 20 April 2015.

18. Phys.org. Efficiency record for flexible CdTe solar cell due to novel polyimide film [online]. 2015.
URL:http://phys.org/news/
2011-06-efficiency-flexible-cdte-solar-cell.html. Accessed: 20 April 2015.

19. Sigma-Aldrich Co. LLC. Organic and Printed Electronics [online]. Helsinki.
URL: http://www.sigmaadrich.com/materials-science/organic-electronics/
opv-tutorial.html. Accessed: 20 April 2015.

20. Halme J, Vahermaa P, Miettunen K, and Lund P. Device physics of dye solar cells. Advanced Materials 2010; 22, 210-234.

21. Evaluate Solar. Solar Power Technology – It's All About the Solar Cell [online].
URL: http://evaluatesolar.com/technology. Accessed: 20 April 2015.

22. Nampalli N. Perovskites:The next PV revolution? [online]. Australia-wide: Solar Choice; 2015.
URL:http://www.solarchoice.net.au/blog/news/perovskites-the-next-solar-pv-revolution-240714. Accessed: 20 April 2015.

23. Abdulrazzaq OA, Saini V, Bourdo S, Dervishi E, Biris AS. Organic Solar Cells: A Review of Materials, Limitations, and Possibilities for Improvement [serial online]. Particulate Science and Technology: An International Journal 2013, 31(5): 427-442.
URL: http://www.tandfonline.com/doi/full/10.1080/02726351.2013.769470. Accessed: 20 April 2015.

24. Solaris Nanosciences Corporation Solar Energy [online]. Providence, Rhode Island: 2005.
URL: http://www.solarisnano.com/solarenergy.php. Accessed: 20 April 2015.

25. Greneir MT, Chai L, and Lu ZH. Organic Photovoltaic: Transition metal oxides increase organic solar-cell power conversion [online]. Tulsa, Oklahoma: Laser Focus World; 6 January 2012.
URL: http://www.laserfocusworld.com/articles/print/volume-48/issue-06/features/transition-metal-oxides-increase-organic-solar-cell-power-conversion.html. Accessed: 20 April 2015.

26. Thomas B. Research [online]. Cambridge MA: Massachusetts Institute of Technology; 2015
URL: http://nanocluster.mit.edu/research.php. Accessed: 20 April 2015.

27. IOP Publishing. Ultrathin solar cell is efficient and easy to make [online]. Bristol UK: 30 September 2013.
URL: http://physicsworld.com/cws/article/news/2013/sep/30/ultrathin-solar-cell- is-efficient-and-easy-to-make. Accessed: 20 April 2015.

28. TiO2 Coated Test Cell Glass Electrodes (Opaque) [online]. DyeSol Ltd.
URL: http://www.dyesol.com/products/tio2-glass-electrodes-opaque.html. Accessed: 22 April 2015.

29. Curtis CJ, Hest MV, Miedaner A, Kaydanova T, Smith L, Ginley DS. Multi-Layer Inkjet Printed Contacts for Silicon Solar Cells [online]. National Renewable Energy Laboratory [NREL], Waikola, Hawaii: IEEE 4th World Conference on Photovoltaic Energy Conversion (WCPEC-4); May 2006.
URL: http://www.nrel.gov/docs/fy06osti/39902.pdf. Accessed: 20 April 2015.

30. Quick D. Researchers cut waste and lower cost of 'CIGS' solar cells using inkjet printing technology [online]. Gizmag; 28 June 2011. URL: http://www.gizmag.com/inkjet-printing-cigs-solar-cells/19057. Accessed: 20 April 2015.

31. Takimiya K. Organic Field Effect Transistors Based on DNTT and Related Organic Semiconductors [online]. Helsinki: Sigma-Aldrich; 2015. URL:http://www.sigmaaldrich.com/materials-science/organic-electronics/dntt-based-organic-semiconductors.html. Accessed: 20 April 2015.

32. Jung S, Sou A, Banger K, Doo-Hyun K, Philip, Chow CY, McNeil CR, Sirringhaus H. All-Inkjet-Printed, All-Air-Processed Solar Cells. Advanced Energy Materials 2014; 4(14): 1-9.

33. Lin YL, Hsu CY, Tai CL. Inkjet Printing Technology for Dye-Sensitized Solar Cells. Advanced materials Research 2012; 476(478):1767- 1770.

34. Chandler DL. While you're up, print me the solar cell [online]. Cambridge Massachussetts; 11 July 2011. URL:http://newsoffice.mit.edu/2011/printable-solar-cells-0711. Accessed: 20 April 2015.

35. Poulain G, Boulord C, Blanc D, Kaminski A, Gautheir M, Dubois C, Semmache B, Lemiti M. Direct laser printing for high efficiency silicon solar cells Fabrication. Applied Surface Science 2011, 257(12): 5241-5244.

36. Gebhardt M, Allenstein F, Hänel J, Scholz C, Clair M. Laser Structuring of Flexible Organic Solar Cells [serial online]. Laser Technik Journal 2013, 10(1): 25-28. URL: http://onlinelibrary.wiley.com/doi/10.1002/latj.201390004/pdf. Accessed: 20 April 2015.

37. Li G, Zhu R, Yang Y. Polymer Solar Cells. Nature Photonics 2012, 6: 153-161. URL: http://yylab.seas.ucla.edu/papers/nphoton.2012.11.pdf. Accessed: 20 April 2015.

38. Liu Y, Chen CC, Hong Z, Gao J, Yang Y, Zhou H, Dou L, Li G, Yang Y. Solution-processed small-molecule solar cells: breaking the 10% power conversion efficiency. Scientific Report 2013; 3, 1- 8. URL:http://www.nature.com/srep/2013/131128/srep03356/pdf/srep03356.pdf. Accessed: 20 April 2015.

39. Liu M, Johnston MB, Snaith HJ. Efficient Planar heterojunction persivskite solar cells by vapour deposition [online]. Macmillan Publishers Limited 2013; 501, 395-398. URL:http://limno.epfl.ch/files/content/sites/limno/files/che600/2014/5.pdf. Accessed: 20 April 2015.

40. Ding KI, Melas-Kyriazi J, Cevey-Ha NL, Chittibabu G. Zakeeruddin SM, Grätzel M, McGehee MD. Deposition of hole-transport materials in solid-state dye-sensitized solar cells by doctor-blading. Organic electronics 2010; 11, 1217-1222.

41. Roldán-Carmona C, Malinkiewicz O, Betancur R, Longo G, Momblona C, Jaramillo F, Camacho L, Bolink HJ. High efficiency single-junction semi-transparent perovskite solar cells [online]. Electronic SupplementaryMaterial (ESI) for Energy & Environmental Science. URL:http://www.rsc.org/suppdata/ee/c4/c4ee01389a/c4ee01389a1.pdf. Accessed 20.04.2015.

42. Mader C, Müller J, Gatz S, Dullweber, Brendel, Rear-Side Point-Contacts by Inline Thermal Evaporation of almunium [online]. Germany: Institute for Solar Energy Research Hamelin (ISFH) and the Solar thermal department of the Institute for SolidState Physics Hanover. URL: http://www.isfh.de/institut_solarforschung/files/ 35ieee_mader.pdf. Accessed: 20 April 2015.

43. Faber R, Zhang K, Large Linear Copper Thermal Evaporation Source for CIGS Solar Applications [online]. MA USA: Vacuum Process Technology, LLC. URL:http://www.vptec.com/documents/ VPTVaporSourceforCIGS_000.pdf. Accessed 20 April 2015.

44. Dr. Witte W, Spiering S, Dr. Dimitrios H. Substitution of the CdS buff er layer in CIGS thin-film solar cells. Vakuum in Forschung und Praxis 2014; 26(1): 23-27.

45. Babkair SS. Charge transport mechanism and device parameters of CdS/CdTe solar cells fabricated by thermal evaporation. Journal of King Abdulaziz University (JKAU) 2010; 22 (1): 21-33. URL: http://nano-center.kau.edu.sa/ Pages-CV-Dr-Saeed-Salem- Babkair.aspx. Accessed: 22 April 2014.

46. Daniel. Methods for manufacturing CZTS optical absorption layers [online]. Gyeonggi-do: SNE Research; September 2011. URL: http://www.sneresearch.com/eng/info/ show.php?c_id=4970&pg=5&s_sort=&su b_cat=&s_type=&s_word=. Accessed: 20 April 2015.

47. Compaan AD, Gupta A, Lee S, Wang S, Drayton J. High efficiency, magnetron sputtered CdS/CdTe solar cells [online]. Solar Energy 2004; 77(6): 815-822. URL:http://www.sciencedirect.com/science/article/pii/ S0038092X04001525. Accessed: 20 April 2015

48. Gupta A, Compann AD. All-sputtered 14% CdS/CdTe thin-film solar cell with ZnO:Al transparent conducting oxide [online]. Applied Physics Letter; 2004.
URL:http://scitation.aip.org/content/aip/journal/apl/85/4/10.1063/1.1775289. Accessed: 20 April 2015.

49. Da Cunha AF, Rudmann D, Salomé P.MP, Kurdesau F. Growth and Characterization of CIGS Solar Cells by RF Magnetron Sputtering With Continous Se Evaporation and End point Detection [online]. Academia edu.
URL:https://www.academia.edu/188944/Growth_and_Characterization_of_CIGS_Solar_Cells_by_RF_magnetron_sputtering_with_continuous_Se_evaporation_and _End_Point_Detection. Accessed: 20 April 2015.

50. Jagannathan B. Properties of sputtered amorphous silicon/crystalline sili con solar cells [serial online]. Washington, DC: IEEE; May 1996; 533 – 536.
URL:http://ieeexplore.ieee.org/xpls/abs_all.jsp?arnumber=564061&tag=1. Accessed: 20 April 2015.

51. Miettunen K, Asghar I, Ruan X, Halme J, Saukkonen T, Lund P. Stabiliza tion of metal counter electrodes for dye solar cells [serial online]. Journal of Electroanalytical Chemistry 2011; 653, 93-99.
URL:http://libra.msra.cn/Publication/49641215/stabilization-of-metal-counter- elec trodes-for-dye-solar-cells.
Accessed: 20 April 2015.

52. Zhi-Hui F, Yan.Bing H, Quan-Min S, Li-Fang Q, Yan L, Lei Z, Xiao-Jun L, Feng T, Yong-Sheng W, Rui-dong X. Polymer solar cells based on a PEDOT: PSS layer spin-coated under the action of an electric field [online]. Chinese Physics B 2009.
URL:http://iopscience.iop.org/16741056/19/3/038601/pdf/16741056_19_3_038601.pdf. Accessed: 20 April 2015.

53. He C, He Q, He Y, Li Y, Bai F, Yang C, Ding Y, Wang L, Ye J.
Organic solar Cells based on the Spin-coated blend films of TPA-th-TPA and PCBM [serial online]. Solar Energy Materials and Solar Cells 2014; 90 (12): 1815-1827.
URL:http://www.sciencedirect.com/science/article/pii/S0927024805003533. Accessed: 20 April 2015.

54. Bae HS, Kim C, Rhee I, Jo HJ, Kim DH, Hong S. Enhancement of the CIGS solar cell's efficiency by anti-reflection coating with Teflon AF [serial online]. Springer 2014; 65(10):1517-1519.
URL:http://link.springer.com/article/10.3938/jkps.65.1517#page-1. Accessed: 20 April 2015.

55. Yoon W, Foos EE, Lumb MP, JG Tischler. Solution processing of CdTe nanocrystals for thin-film solar cells [serial online]. Austin TX: IEEE 3-8 June 2012; 002621-002624.
URL:http://ieeexplore.ieee.org/stamp/
stamp.jsp?tp=&arnumber=6318132. Accessed: 21 April 2015.

56. Lee JG, Cheon JH, HS Yang, Lee DK, Kim JH. URL: Enhancement of photovoltaic performance in dye-sensitized solar cells with the spin-coated TiO2 blocking layer [online]. Pubmed 2012.
URL: http://www.ncbi.nlm.nih.gov/pubmed/22966702.
Accessed: 20 April 2015.

57. Creghton JR, Ho P. Introduction to Chemical Vapor Deposition (CVD) [online]. Albuquerque, NM: ASM International 2001.
URL:http://www.asminternational.org/documents/10192/1849770/
ACFAA6 E.pdf. Accessed: 20 April 2015.

58. Faller FR, Hurrle A. High-temperature CVD for crystalline-silicon thin-film solar cells [serial online]. Electron Devices, IEEE Transactions on 2002; 46(10): 2048-2054.
URL:http://ieeexplore.ieee.org/stamp/
stamp.jsp?arnumber=791995. Accessed: 20 April 2015.

59. Kim H, Bae SH, Han TH, Lim KG, Ahn JH, Lee TW. Organic solar cells using CVD-grown graphene electrodes [serial online]. IOP Publishing 2013.
URL: http://iopscience.iop.org/0957-4484/25/1/014012/article.
Accessed: 20 April 2015.

60. Kalita G, Wakita K, Umeno M, Hayashi Y, Tanemura M. Large-area CVD graphene as transparent electrode for efficient organic solar cells. [serial online]. Photovoltaic Specialists Conference (PVSC), 2012 38th IEEE; Austin, Texas. 03137 - 003141
URL: http://ieeexplore.ieee.org/stamp/stamp.jsp?arnumber=6318244.
Accessed: 20 April 2015.

61. Romeo A, Terheggen M, Ras- Abou D, Bätzner D.L, Haug F-J, Kälin M, Rudmann D, Tiwari AN. Development of Thin-film Cu (In,Ga)Se_2 and CdTe Solar Cells [serial online]. Progress in Photovoltaic Research and Application. Zurich, Switzerland: John Wiley & Sons 2004.
URL:http://profs.scienze.univr.it/~romeo/Publications/
ProgPV_v12_i2-3_03.pdf Accessed: 20 April 2015.

62. Dr.Valvoda V, Dr. Toušková J, Dr. Kindl D. Electrochemical Deposition of CdTe Layers. Their Structure and Electrical Properties [serial online]. Crystal Research and Technology 2006; 21(8) 975–981.
URL:http://onlinelibrary.wiley.com/doi/10.1002/crat.2170210803/
abstract. Accessed: 20 April 2015.

63. Pazoki M, Taghavinia N, Abdi Y, Tajabadi F, Boschloo G, Hagfeldt A.CVD-grown TiO_2 particles as light scattering structures in dye-sensitized solar cells. RSC Advances 2012. URL:http://pubs.rsc.org/en/Content/ArticleLanding/2012/RA/c2ra21361c#!divAbstract. Accessed: 20 April 2015.

64. Tutorial 2-Chemical Vapor Deposition [online]. Precision Fabricator. Stoughton, MA: Rice University. URL: http://www.precisionfab.net/tutorials02.aspx. Accessed: 20 April 2015.

65. Photolithography [online]. Georgia Institute of Technology. URL: http://www.ece.gatech.edu/research/labs/vc/theory/photolith.html. Accessed: 20 April 2015.

66. Photolithography Background [online]. Madison WI: UW MRSEC Education Group 2015. URL: http://education.mrsec.wisc.edu/476.htm. Accessed: 20 April 2015.

67. Saga T. Advances in Crystalline silicon solar cells technology for industry al mass production [online]. Macmillan 2010. URL: http://www.nature.com/am/journal/v2/n3/full/am201082a.html. Accessed: 20 April 2015.

68. Optics InfoBase, official website. URL: http://www.opticsinfobase.org/view_article.cfm. Accessed: 20 April 2015.

69. Wang BL. Stamp fabrication by step and stamp nanoimpriting dissertation [online]. New Big Future Inc 26 May 2011. URL: http://nextbigfuture.com/2011/05/stamp-fabrication-by-step-and- stamp.html. Accessed: 20 April 2015.

70. Lan H, Ding Y. Nanoimprint Lithogrpahy [online]. Croatia: Intech; February 2010. URL: http://cdn.intechopen.com/pdfs-wm/8680.pdf. Accessed: 21 April 2015.

71. Mellor A, Hauser H, Wellens C, Benick J, Eisenlohr J, Peters M, Guttowski A, Tobías I, Martí A, Luque A, Bläsi B. Nanoimprinted Diffraction grating for rystalline silicon solar cells: implementation characterization and simulation [online]. Optics Express 11 March 2013; 21: A295-A304. URL:http://www.opticsinfobase.org/oe/abstract.cfm?uri=oe-21-S2-A295. Accessed: 21April 2015.

72. Battaglia C, Escarré J, Söderström K, Erni L, Ding L, Bugnon G, Billet A, Bocard M. Barraud L, Wolf SD, Haug FJ, Despeisse M, Ballif C. Nanoimprint Lithography for High- Efficiency Thin-film Silicon Solar Cells [serial online]. Neuchâtel, Switzerland: Nano Letter 2011; 11(2): 661-665. URL: http://pubs.acs.org/doi/abs/10.1021/nl1037787. Accessed: 21 April 2015.

73. Yang Y, Mieiczarek K, Aryal M, Zakhidov A, Hu W. Nanoimprinted [serial online]. ACS Nano 2012; 6(4): 2877-2892. URL: http://pubs.acs.org/doi/abs/10.1021/nn3001388. Accessed: 21 April 2015.

74. Berger M. Nanoimprint lithography for the fabrication of efficient low band gap polymer solar cells [online]. Nano werk; 12 November 2014. URL: http://www.nanowerk.com/spotlight/ spotid=38076.php. Accessed: 21 April 2015.

75. Electrophotography [online]. My Print Guide. International Paper. URL: http://www.myprintguide.org/glossary/ definition.php?term=Electrophotography+%28EP%29. Accessed: 21April 2015.

76. Sauers, RR. Organic dyes for photovoltaic cells and for photoconductive electrophotography systems [online]. US Patent. Highland Park, NJ: Patexia. Research; October 2001. URL: https://www.patexia.com/us-patents/06307147/claims. Accessed: 21 April 2015.

77. Smith D. Which Laminator should I Choose? [online]. Wales, England: Vivid Laminating Technologies 2015. URL: http://www.vivid-online.com/which_laminator. Accessed: 21 April 2015.

78. Solar Module Optimisation with PVB Film- Solar Technology in Perfection [online]. Product and Services. Trosifol; October 2012. URL:http://www.kuraray.us.com/wp-content/uploads/2013/03/ TROSIFOL- Solar-Technical-.pdf. Accessed: 21 April 2015.

79. Bear JH. Sheet- fed Press [online]. About Tech. URL: http://desktoppub.about.com/cs/printing/g/sheetfedpress.htm. Accessed: 21 April 2015.

80. York Andy, Brochure Printing -web or sheet-fed? [online]. Bourne, Lincolnshire: Warner Midlands PLC; January 2014. URL: http://www.warners.co.uk/Blog/301/ Brochure_Printing_-_web_or_sheet- fed/. Accessed: 21 April 2015.

81. How To Choose Between Web Vs. Sheetfed Printing [online]. Direct Mail Insider; Ocotober 2010.
URL:http://www.directmailinsider.com/
how-to-choose-between-web-vs-sheetfed-printing/.
Accessed: 21 April 2015.

82. Printable NanoChromics Technology from NTERA [online]. Package Printing; June 2010.
URL:http://www.packageprinting.com/article/
new-developments- technologies-package-printers-ntera-tagsys/1/.
Accessed: 22 April 2015.

83. Clean for Yield [online]. European Funded Research Project.
URL: http://www.clean4yield.eu/partners. Accessed: 22 April 2015.

84. Rardin TE, Xu R. Priting Process Used to Manufacture photovoltaic Solar Cells [online]. The Journal of Technology Studies 2011. 62-68.
URL:http://scholar.lib.vt.edu/ejournals/JOTS/v37/v37n2/pdf/rardin.pdf.
Accessed: 21 April 2015.

85. Solna 425D Sheet Fed Offset Printing Press [online]. Qingdao ZFC Trading, officila website.
URL: http://www.zfc-printing.com/
sell-1240106-solna-425d-sheet-fed-offset- printing-press.html.
Accessed: 21 April 2015.

86. Gravure [online]. PrintWiki-The Free Encyclopedia of Print.
URL: http://printwiki.org/Gravure. Accessed: 21 April 2015.

87. Bear JH. Gravure Priting [online]. About Tech.
URL: http://desktoppub.about.com/cs/printing/g/gravure.htm.
Accessed: 21 April 2015.

88. Kopola P, Aemouts T, Guillerez S, Jin H, Tuomikoski M, Manninen A, Hast J. High efficient plastic solar cells fabricated with a high-throughput gravure printing method [serial online]. Solar energy Material and Solar Cells 2010; 94(10): 1673-1680.
URL:http://www.sciencedirect.com/science/article/pii/
S0927024810003211. Accessed: 21 April 2015.

89. Printing Industry[online]. Illinois Sustainable Technology Center.
URL:http://www.istc.illinois.edu/info/library_docs/manuals/printing/
gravure.htm. Accessed: 21 April 2015.

90. Commercial-Web Printing [online]. Baldwin, official website.
URL: http://www.baldwintech.com/en/product_segments/
commercial_web_systems.aspx. Accessed: 21 April 2015.

91. Solar Module Production Line [online]. Xinology Co., Ltd. Official website URL: http://xinology.com:888/ Glass-Processing-Equipments-Supplies-Consumables/ glass-photovoltaic/solar-module-production-line/features-specs/ solar-module-laminating-inspection.html. Accessed: 21 April 2015.

92. Roll laminator machine [online]. Bright office Stationary, official website. URL:http://www.brightstationery.com/english/ products.asp?classcode=122. Accessed: 21 April 2015.

93. What is 3D priting? [online]. 3D Priting.com 2015. URL: http://3dprinting.com/what-is-3d-printing/. Accessed: 21 April 2015.

94. Lucero T. Could 3D Printing Utterly Change Solar Panel [online]. Energy Digital; March 2015. URL: http://www.energydigital.com/greentech/3793/ Could-3D-Printing- Utterly- Change-Solar-Panel-Technology. Accessed: 21 April 2015.

95. Halterman T. Solar Power, Organic Photovoltaics And 3d Printing [online]. 3D Printer World; March 2014. URL:http://www.3dprinterworld.com/article/ solar-power-organic-photovoltaics-and-3d-printing. Accessed: 21 April 2015.

96. Millsaps BB. The Sky's the Limit for the 3D Printing of Solar Panels at Australia's VICOSC [online]. 3D Print.com; 11 September 2014. URL: http://3dprint.com/14885/3d-printing-solar-panels/. Accessed: 21 April 2015.

97. 3D Printed Solar Energy Trees [online]. Alternate Energy 28 February. URL: http://www.alternative-energy-news.info/3d-printed-solar-energy-trees. Accessed: 21 April 2015.

98. Edward T. Japanese Breakthrough & 3D Printing Could Make Wireless Transmission of Solar Energy a Reality [online]. 3D Print.com; 18 March 2015. URL: http://3dprint.com/50832/jaxa-3d-printed-solar-energy/. Accessed: 21 April 2015.

99. 3D Printers [online]. Amazon Official Website. URL:http://www.amazon.com/Best-Sellers-Industrial-Scientific 3DPrinters/zgbs/industrial/6066127011. Accessed: 21 April 2015.

100. VTT Technical Research Centre of Finland Ltd, official website. Espoo, Finland URL:http://www.vttresearch.com/media/news/ solar-power-from-energy-harvesting-trees-—-watch-the-video. Accessed: 21 April 2015.

101. Informer Technologies, Inc. official website [online].
URL: http://agilent-vee-pro.software.informer.com/screenshot/318865/.
Accessed: 21 April 2015.

Appendix 1: Matlab Software Code for Calculating Solar Cell Efficiency

```
clc;
n=1;


a1=load('EL01_02_01_8mar.txt');


data1=zeros(n,4);


for j=1:n

V=Vk(:,j);
I=Ik(:,j);
A=3.5;
mismatch=1.06348;
P=100;

%[] = IV(V, I, A, mismatch, P)
%Computes the parameters of an IV-curve. Input: V = voltage
(V),
%I = current (A), A = active area of the cell (cm2),
%mismatch = mismatch-factor of the simulator (no dimen-
sion),
%P = power of the incident light, (usually) 100 (mW/cm2).
%Output: P_mpp (mW/cm2), V_mpp (V), I_mpp (mA/cm2),
%I_sc (mA/cm2),V_oc (V), FF (%), nyy (%).



I_density=(-I./A)*1000*mismatch;
P_density=V.*I_density;
```

```
P_mpp=max(P_density);

%tunnistetaan kuinka mones mittauspiste vastaa maksimiteho-
pistettä

index=[];
    for i=1:length(P_density),
        if P_density(i)==P_mpp, index=i;
        else i=i+1;
        end
    end



V_mpp=V(index);
I_mpp=I_density(index);



I_sc=[];
V_oc=[];
I_posit=[];
V_negat=[];
    for i=1:length(V),
        if V(i)<0, V_negat(i)=V(i);
        else break
        end
    end
       index_negat_V=length(V_negat);
       index_posit_V=length(V_negat)+1;



       dV=V(index_posit_V)-V(index_negat_V);
```

```
       dI=I_density(index_posit_V)-I_density(in-
dex_negat_V);

       k=dI/dV;

       I_sc=I_density(index_negat_V)+k*(-V(index_negat_V))


     for iii=1:length(I_density),
        if I_density(iii)>0, I_posit(iii)=I_density(iii);
        else break
        end
     end
       index_posit_I=length(I_posit);
       index_negat_I=length(I_posit)+1;

 dV=V(index_posit_I)-V(index_negat_I);
       dI=I_density(index_posit_I)-I_density(index_ne-
gat_I);

       k=dV/dI;

       V_oc=V(index_posit_I)-k*I_density(index_posit_I);



 FF=((V_mpp*I_mpp)/(V_oc*I_sc))*100;

 nyy=((V_mpp*I_mpp)/P)*100;



plot(V,I_density,V,P_density),
```

```
xmin=-0.2;xmax=0.8;ymin=-1;ymax=max(I_density)+3;axis([xmin
xmax ymin ymax])
 xlabel('Voltage(V)'),ylabel('Current density / power den-
sity (mA/cm^2) / (mW/cm^2)')
 grid
hold on;

data=[I_sc, V_oc, FF, nyy]



data1(j,:)=data;

end
data1

dlmwrite('kenno-x-y-z.txt', data1);
```

Appendix 2: Photographs of the Prototype Solar Cells Manufactured in this Project

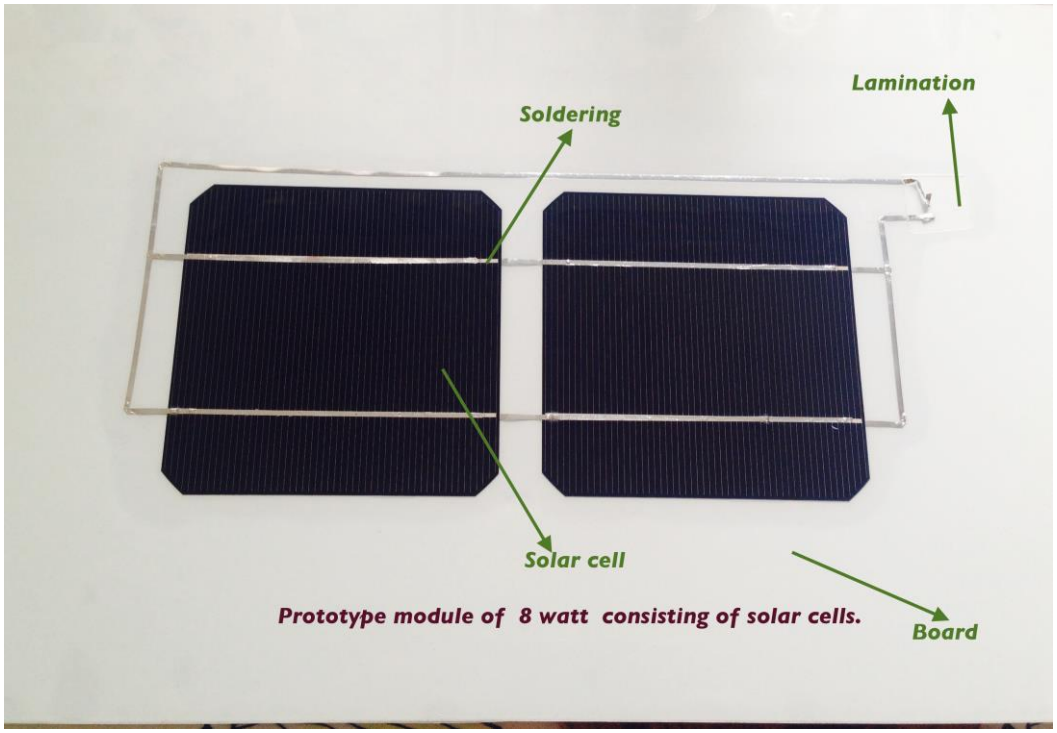

Figure A1: (The) photographs of multi-crystalline silicon solar cells.

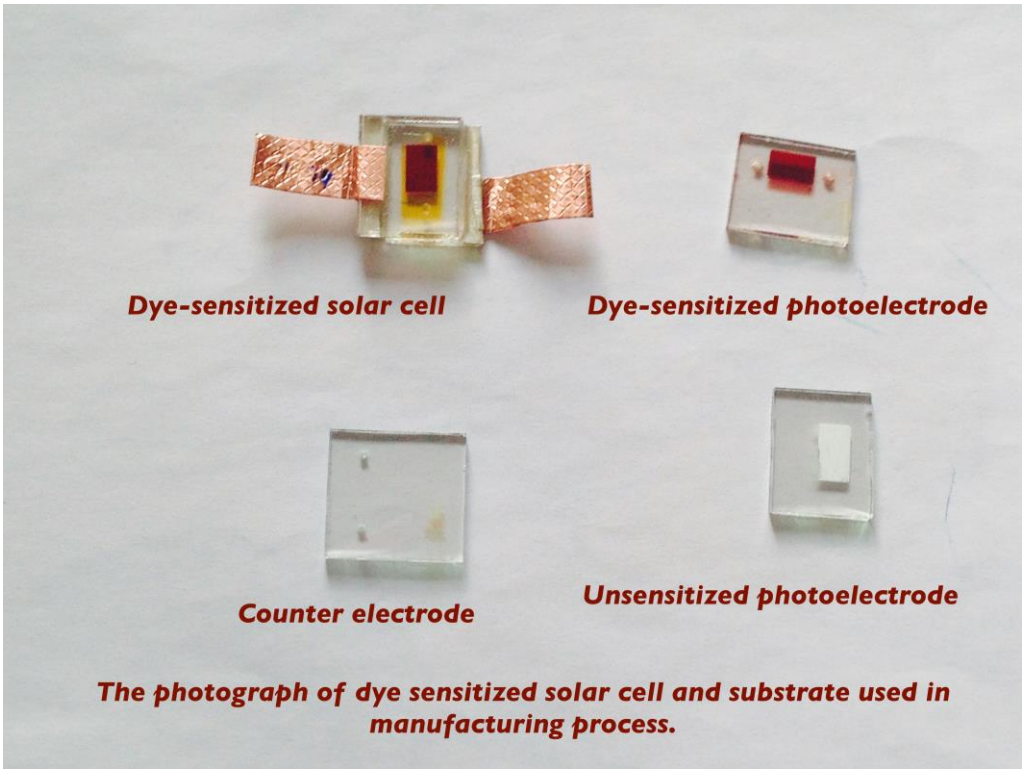

Figure A2: (The) photographs of a Dye-sensitized solar cell.

Appendix 3: Screenshot of the Agilent VEE Pro Software Programme

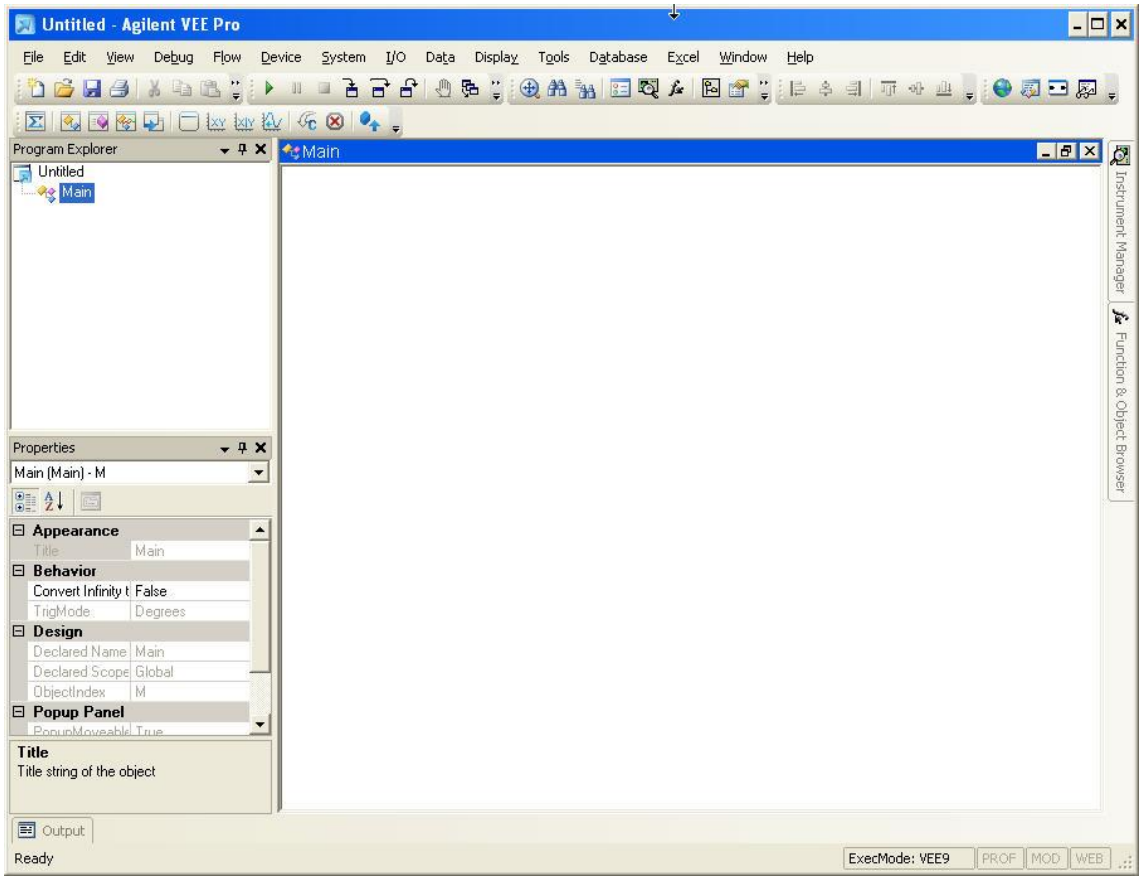

Figure A3: Screenshot of Agilent VEE Pro software programme. Reprinted from Agilent VEE Pro website [101].